Electronic Supplementary Material (ESI) for CrystEngComm
This journal is © The Royal Society of Chemistry 2011

Electronic Supplementary Information for MS:

A series of novel entangled coordination frameworks with inherent features of self-threading, polyrotaxane and polycatenane

Haiyan Chen,[a] Dongrong Xiao,*[a] Jianghong He,[a] Zhifu Li,[a] Guangju Zhang,[a] Dianzhen Sun,[a] Ruo Yuan,[a] Enbo Wang*[b] and Qun-Li Luo*[a]

[a] *College of Chemistry and Chemical Engineering, Southwest University, Chongqing, 400715, P. R. China. E-mail: xiaodr98@yahoo.com.cn*

[b] *Key Laboratory of Polyoxometalate Science of Ministry of Education, Department of Chemistry, Northeast Normal University, Changchun, 130024, P. R. China*

Table S1. Selected bond lengths [Å] for compounds **1–6**

Compound **1**			
Mn(1)-O(3)#1	2.127(3)	Mn(2)-O(2)	2.096(4)
Mn(1)-O(9)#2	2.156(3)	Mn(2)-O(7)	2.111(4)
Mn(1)-O(1)	2.175(4)	Mn(2)-O(4)#1	2.162(4)
Mn(1)-N(3)	2.229(5)	Mn(2)-OW1	2.252(4)
Mn(1)-O(10)#3	2.274(3)	Mn(2)-N(4)#4	2.272(5)
Mn(1)-OW1	2.342(4)	Mn(2)-N(1)	2.301(5)
Compound **2**			
Mn(1)-O(3A)#1	2.022(10)	Mn(2)-O(4A)#2	2.029(7)
Mn(1)-O(3A)#2	2.022(10)	Mn(2)-O(4A)#1	2.029(7)
Mn(1)-O(1)	2.108(4)	Mn(2)-OW1	2.080(4)
Mn(1)-O(1)#3	2.108(4)	Mn(2)-O(2)	2.088(4)
Mn(1)-N(1)	2.161(5)	Mn(2)-O(2)#3	2.088(4)
Mn(1)-O(3)#1	2.264(11)	Mn(2)-O(4)#1	2.203(7)
Mn(1)-O(3)#2	2.264(11)	Mn(2)-O(4)#2	2.203(7)
Compound **3**			
Mn(1)-O(2)#1	2.1169(16)	Mn(2)-O(7)	2.1115(19)
Mn(1)-O(3)#2	2.1210(19)	Mn(2)-O(4)#2	2.1268(18)
Mn(1)-O(1)	2.1304(17)	Mn(2)-OW2	2.176(2)
Mn(1)-O(8)	2.1712(19)	Mn(2)-O(10)#3	2.1921(16)

This journal is © The Royal Society of Chemistry 2011

Mn(1)-O(9)#3	2.2321(16)	Mn(2)-N(1)	2.209(2)
Mn(1)-OW1	2.2368(19)		
Compound **4**			
Ni(1)-O(1)	2.059(2)	Ni(1)-OW1	2.086(2)
Ni(1)-N(1)	2.081(3)	Ni(1)-OW2	2.109(2)
Ni(1)-N(3)	2.084(3)	Ni(1)-O(4)#1	2.171(2)
Compound **5**			
Co(1)-O(1)	2.024(3)	Co(2)-O(3)#2	2.041(3)
Co(1)-O(4)#1	2.062(3)	Co(2)-O(2)	2.080(3)
Co(1)-O(7)	2.108(3)	Co(2)-O(2)#3	2.080(3)
Co(1)-N(1)	2.110(4)	Co(2)-O(7)#3	2.114(3)
Co(1)-N(2)	2.124(4)	Co(2)-O(7)	2.114(3)
Co(2)-O(3)#1	2.041(3)		
Compound **6**			
Ni(1)-N(1)	2.033(4)	Ni(2)-N(8)#3	2.027(4)
Ni(1)-N(4)#1	2.046(4)	Ni(2)-N(5)	2.043(4)
Ni(1)-O(4)#2	2.067(3)	Ni(2)-O(8)#4	2.109(3)
Ni(1)-O(1)	2.104(3)	Ni(2)-O(7)	2.115(3)
Ni(1)-O(2)	2.149(3)	Ni(2)-O(9)#4	2.153(4)
Ni(1)-O(3)#2	2.199(4)	Ni(2)-O(6)	2.166(3)

Symmetry transformations used to generate equivalent atoms: for **1**: #1 x, -y+1/2, z-1/2; #2 x, -y+1/2, z+1/2; #3 -x+1, y-1/2, -z+1/2; #4 x, y+1, z; for **2**: #1 x-1, y, z; #2 x-1, -y+1, z; #3 x, -y+1, z; for **3**: #1 -x+2, -y, -z; #2 x-1, y, z; #3 x+1, y, z; for **4**: #1 -x, -y, -z; for **5**: #1 x, y, z+1; #2 -x, -y, -z-1; #3 -x, -y, -z; for **6**: #1 x+1/2, y-1/2, z; #2 x, -y, z+1/2; #3 x-1/2, y-1/2, z; #4 x-1/2, -y+1/2, z-1/2.

This journal is © The Royal Society of Chemistry 2011

Supporting Figures

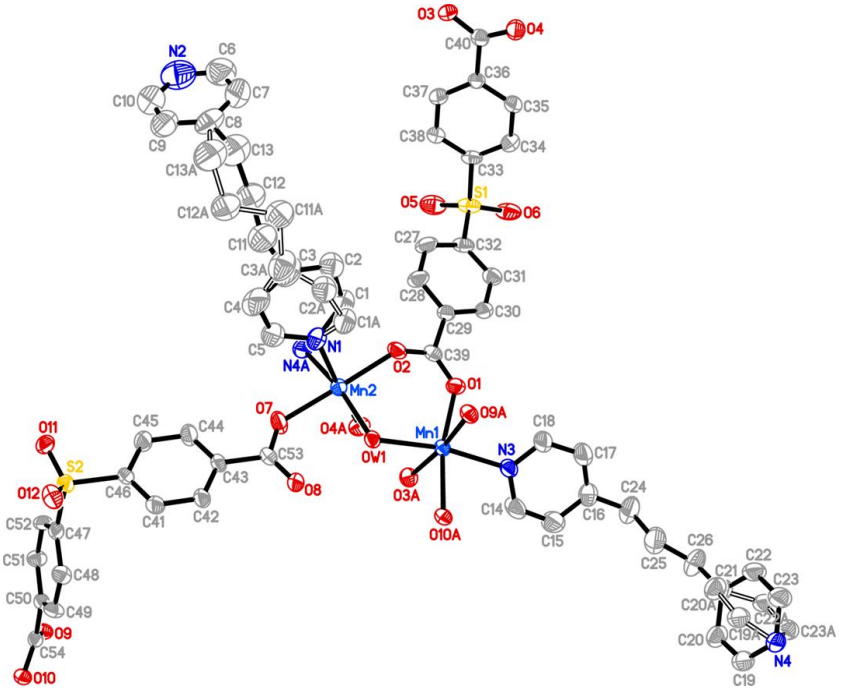

Fig. S1 ORTEP drawing of the coordination environment for Mn atoms in **1** with thermal ellipsoids at the 30% probability level. The hydrogen atoms are omitted for clarity.

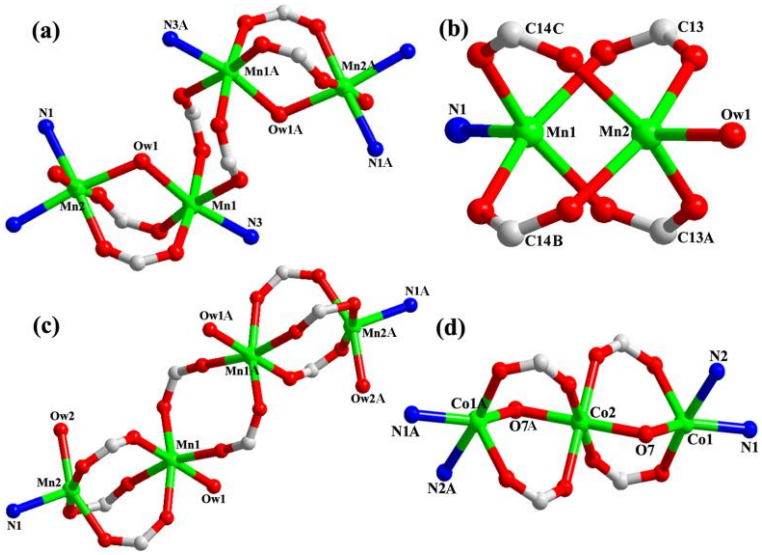

Fig. S2 Schematic representation of inorganic SBUs: (a) the tetranuclear manganese unit of **1**, (b) the dinuclear manganese unit of **2**, (c) the tetranuclear manganese unit of **3**, (d) the trinuclear cobalt unit of **5**. (Symmetry transformations used to generate equivalent atoms: for **1**: A = 1-x, -y, 1-z; for **2**: A = x, 1-y, z; B = -1+x, 1-y, z; C = -1+x, y, z; for **3**: A = 2-x, -y, -z; for **5**: A = -x, -y, -z.)

This journal is © The Royal Society of Chemistry 2011

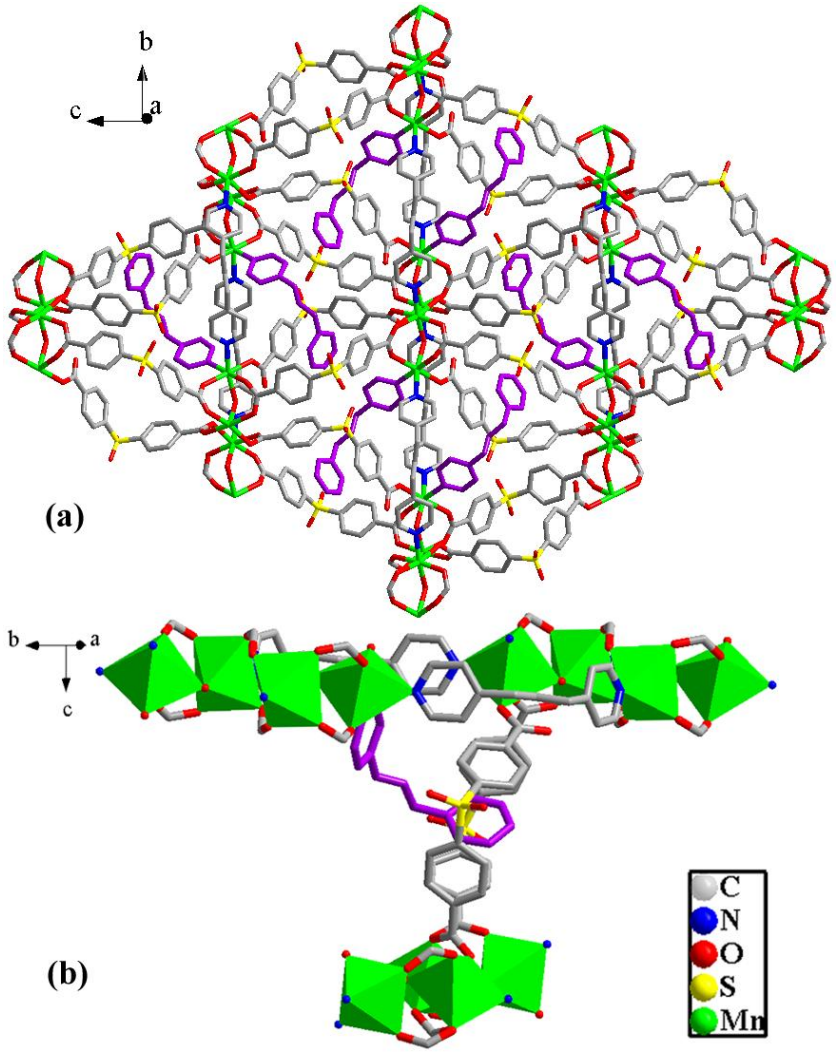

Fig. S3 Perspective views of (a) the 2D self-threading network of **1** and (b) the detail of the self-threading feature in **1**. The one-end coordinated bpp ligands as dangling arms are highlighted by purple.

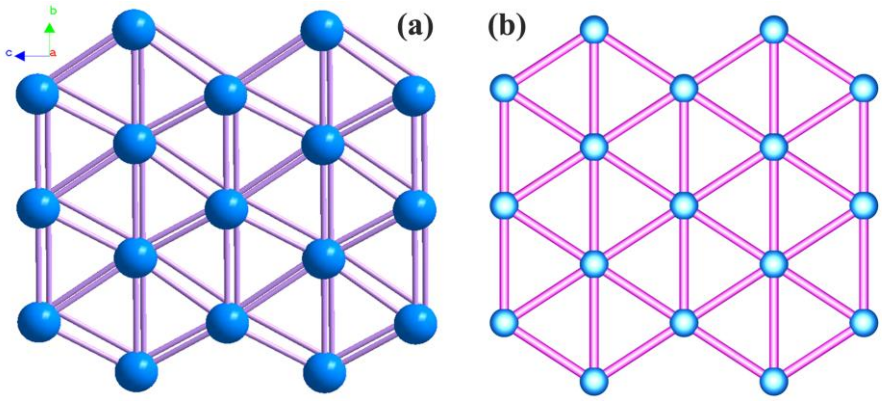

Fig. S4 Schematic representation of (a) the double-edged 2D 3^6-**hxl** net of **1** and (b) the ordinary 2D 3^6-**hxl** network.

This journal is © The Royal Society of Chemistry 2011

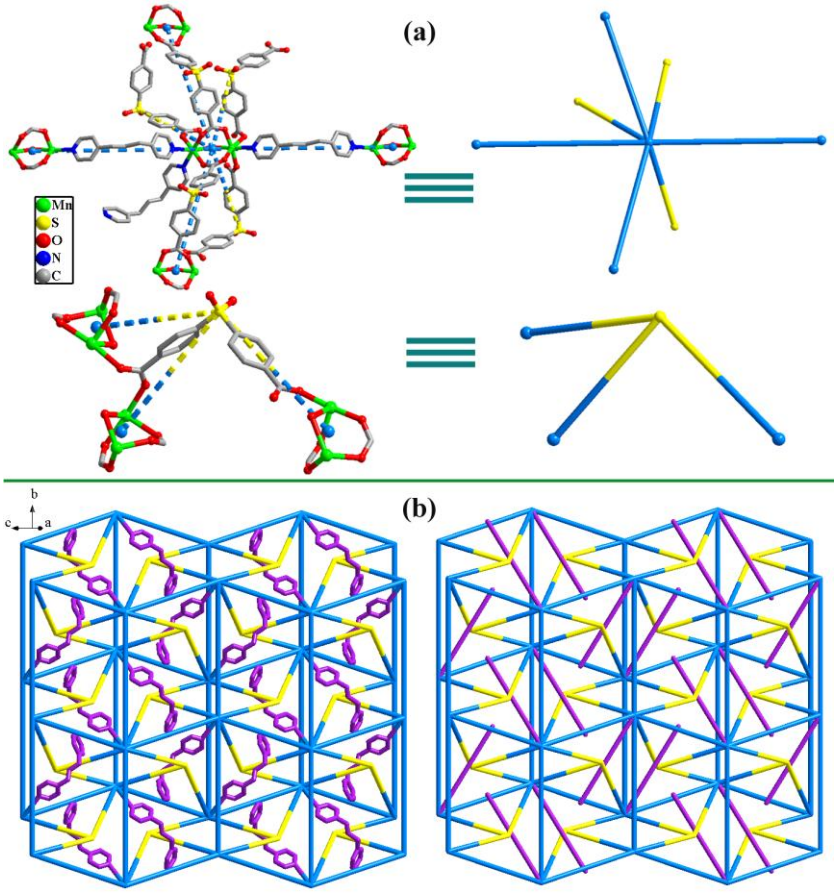

Fig. S5 (a) Perspective (left) and simplified (right) views of the seven-connected dinuclear manganese core and three-connected sdba ligand in **1**. (b) Schematic illustration of the 2D self-threading network with (3,7)-connected (3.4.5)(3^2.4^5.5^7.6^6.7) topology of **1**, in which the one-end coordinated bpp ligands as dangling arms are highlighted by purple.

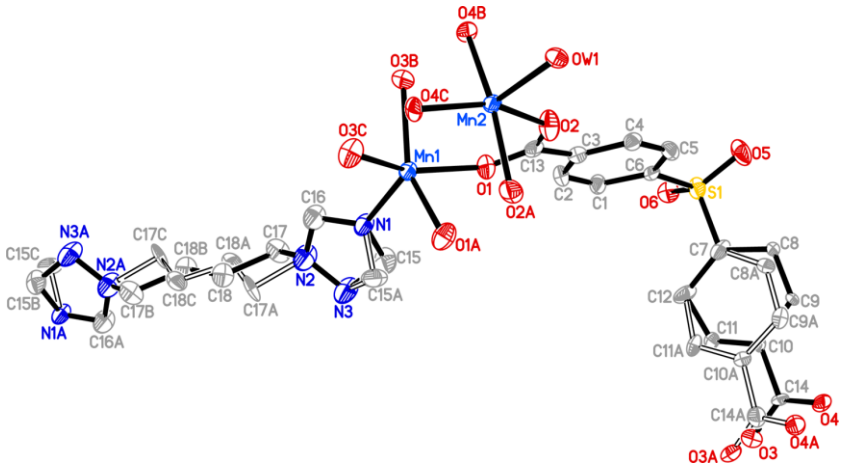

Fig. S6 ORTEP drawing of the coordination environment for Mn atoms in **2** with thermal ellipsoids at the 30% probability level. The hydrogen atoms are omitted for clarity.

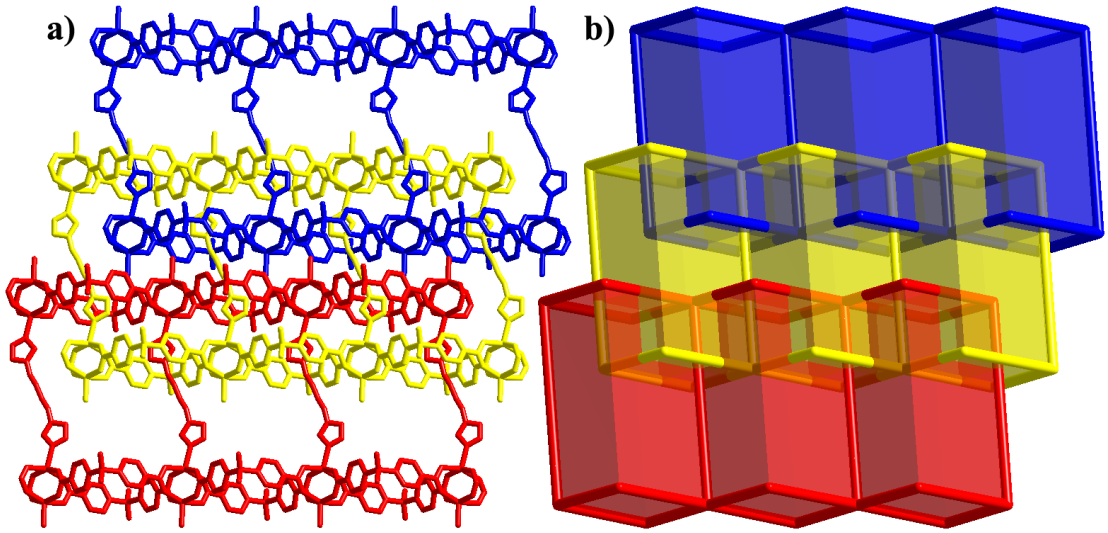

Fig. S7 Perspective (a) and schematic (b) views of the parallel polycatenation of three different 1D quadruple chains in **2**.

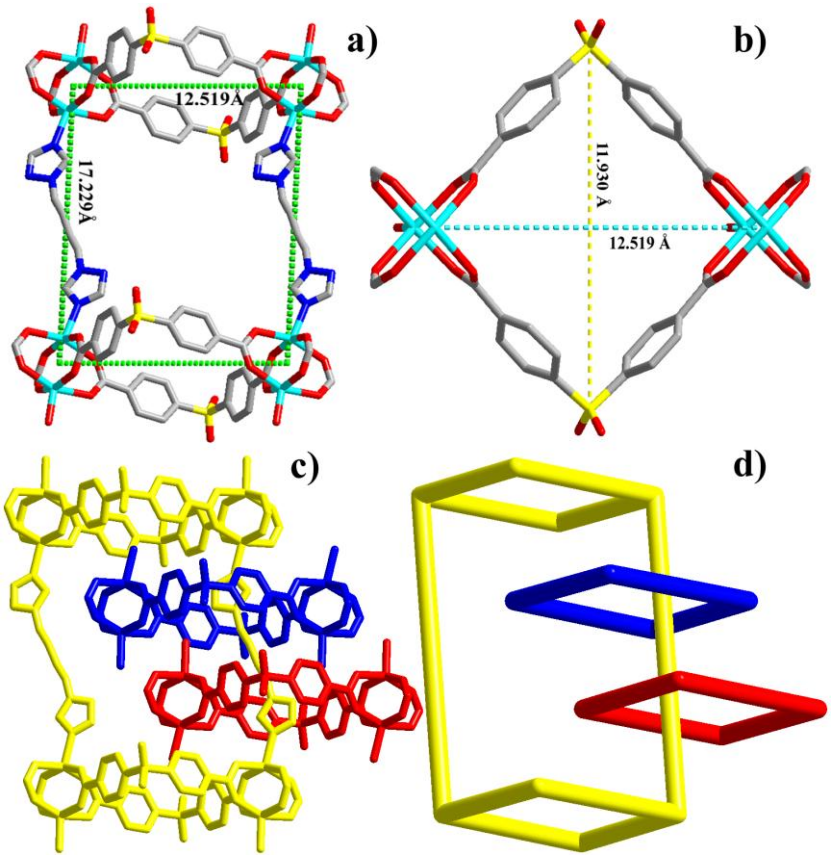

Fig. S8 View of (a) a single tetragonal mesh and (b) a single 2-membered loop $[Mn_4(sdba)_2]$ with the relative dimensions 12.519 × 17.229 Å and 12.519 × 11.930 Å, respectively. Perspective (a) and schematic (b) views of the catenation of the tetragonal mesh with two-membered loops in **2**.

This journal is © The Royal Society of Chemistry 2011

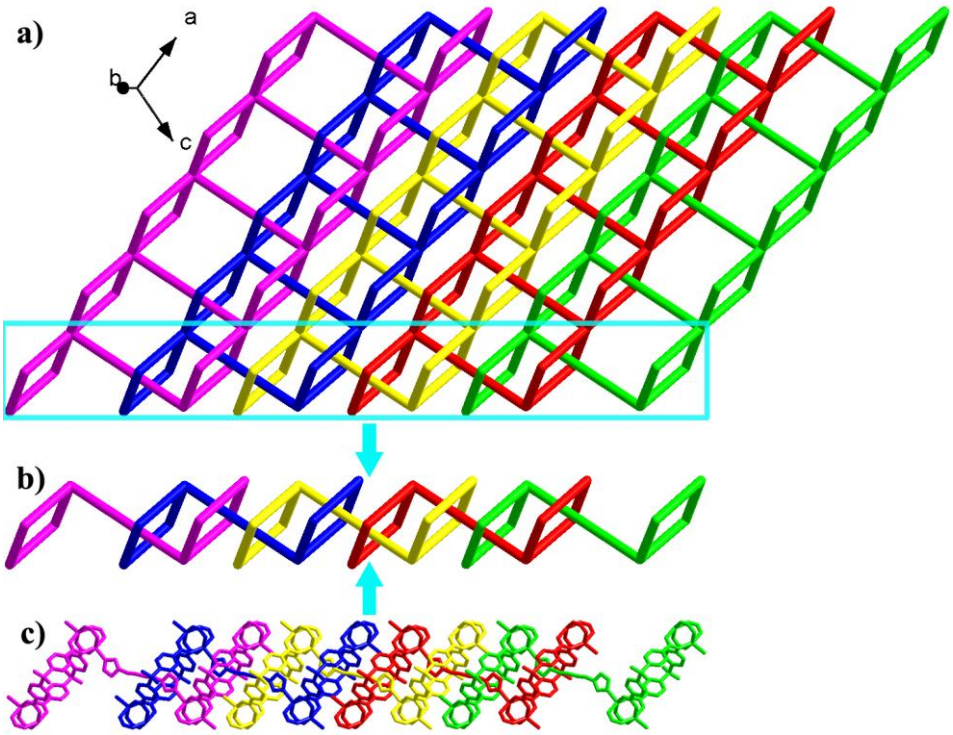

Fig. S9 (a) Schematic view of the overall 2D polycatenated layer of **2**. Schematic (b) and perspective (c) views of the 1D polyrotaxane column of **2**.

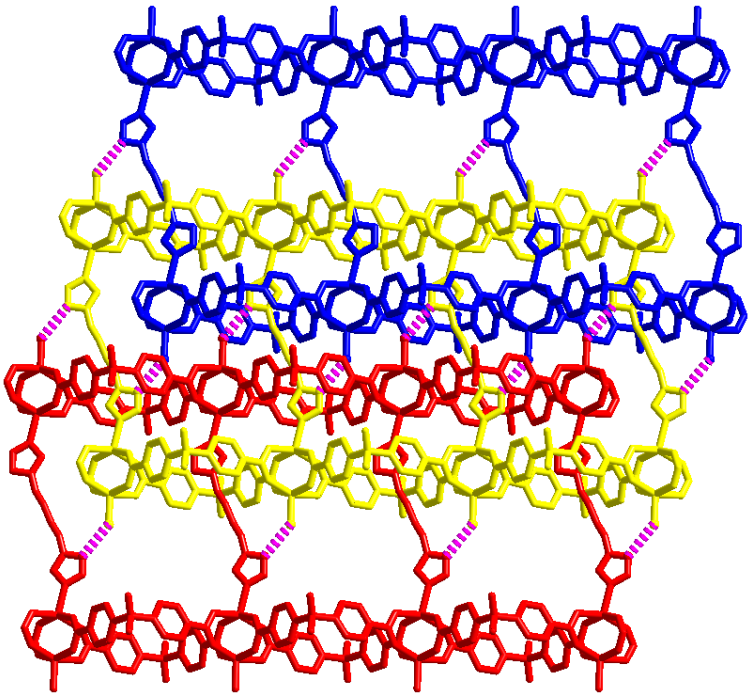

Fig. S10 Perspective view of the hydrogen bonding interactions (Ow(1)···N(3) 2.839 Å) between adjacent 1D quadruple chains of the overall 2D polycatenated layer in **2**. The hydrogen bonds are indicated by purple dashed lines.

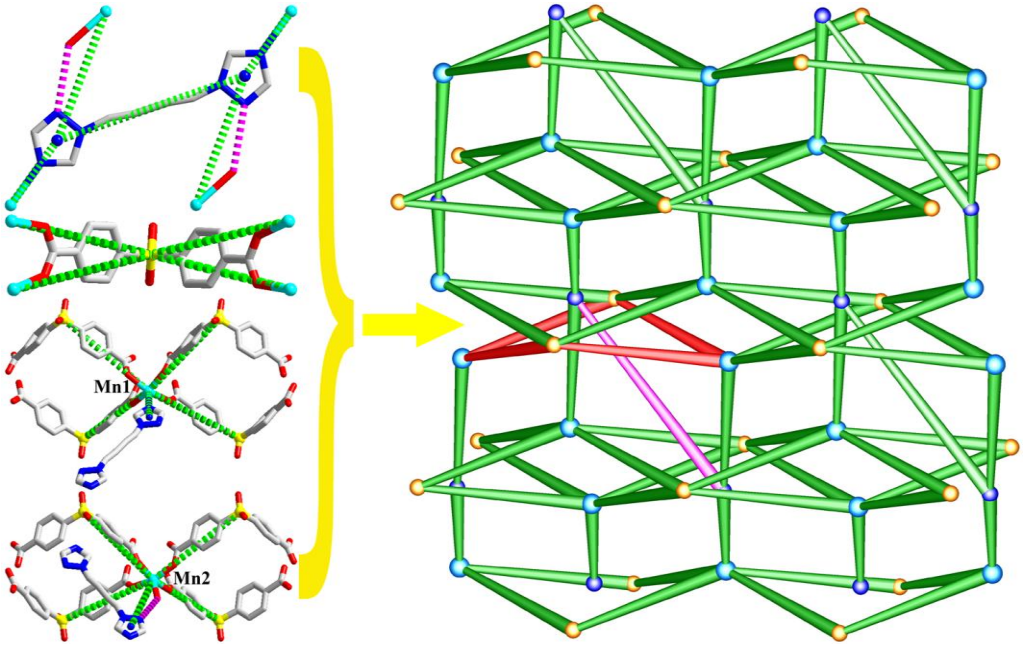

Fig. S11 (left) Perspective views of the three-, four- and five-connected nodes in **2**. Purple dashed lines illustrate the hydrogen bonds, green dashed lines illustrate the circumstance of each node (Mn atoms and sdba ligands). (right) Schematic representation of the trinodal (3,4,5)-connected 2D self-penetrating network of **2** that is formed when hydrogen bonds are taken into account. The four-membered shortest ring is threaded by a rod of the same net, illustrating that this net is a self-penetrating one.

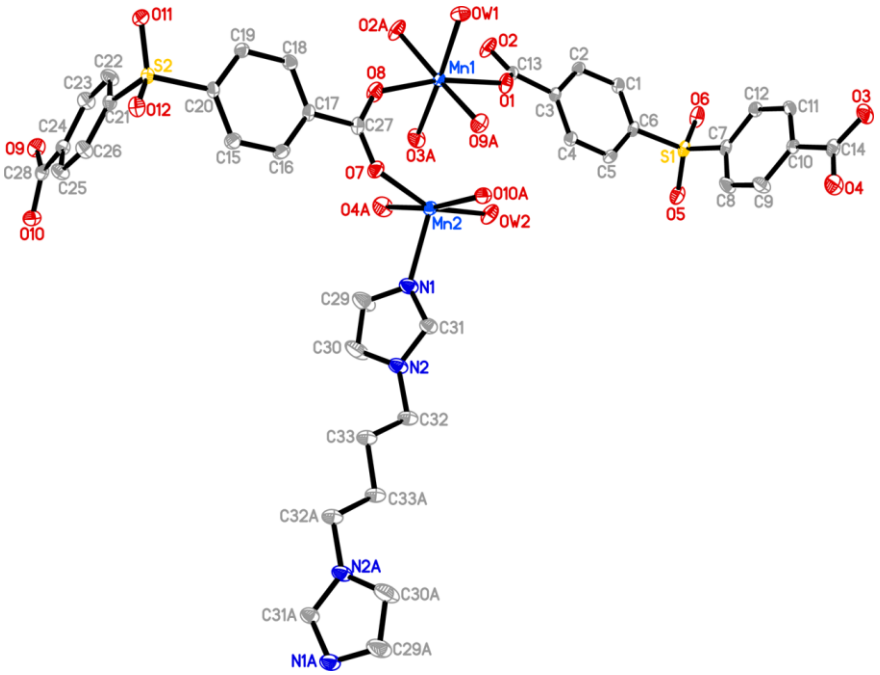

Fig. S12 ORTEP drawing of the coordination environment for Mn atoms in **3** with

thermal ellipsoids at the 30% probability level. The isolated water molecules and hydrogen atoms are omitted for clarity.

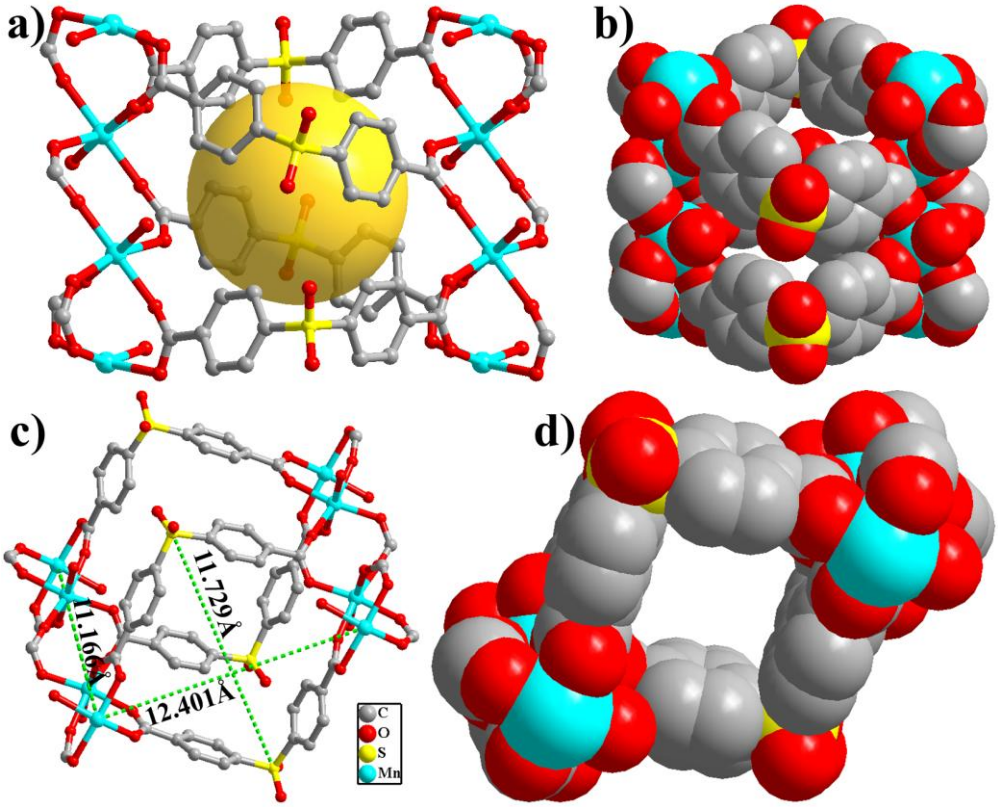

Fig. S13 Perspective (a, c) and space-filling (b, d) views of a single cuboidal cage of **3** with the relative dimensions 12.401 × 11.729 × 11.166 Å, highlighting the large cavity.

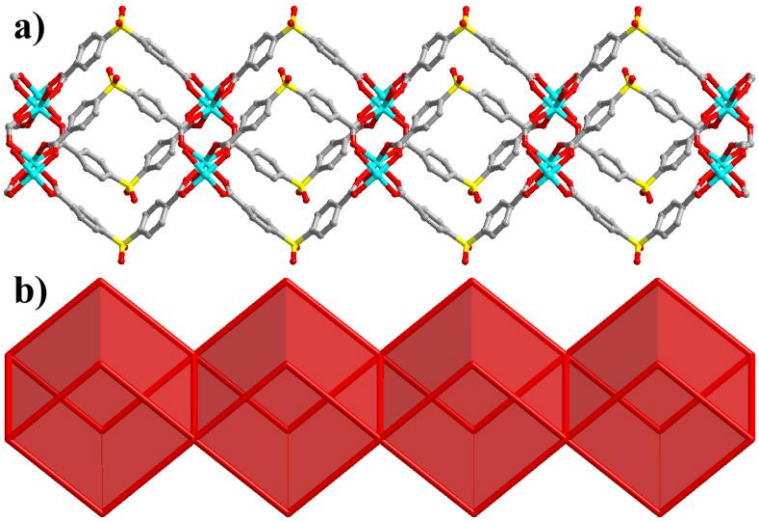

Fig. S14 Perspective (a) and schematic (b) views of the 1D quadruple chains of **3**, which is formed by the cuboidal cages with cage-to-cage connections in an edge-sharing mode.

This journal is © The Royal Society of Chemistry 2011

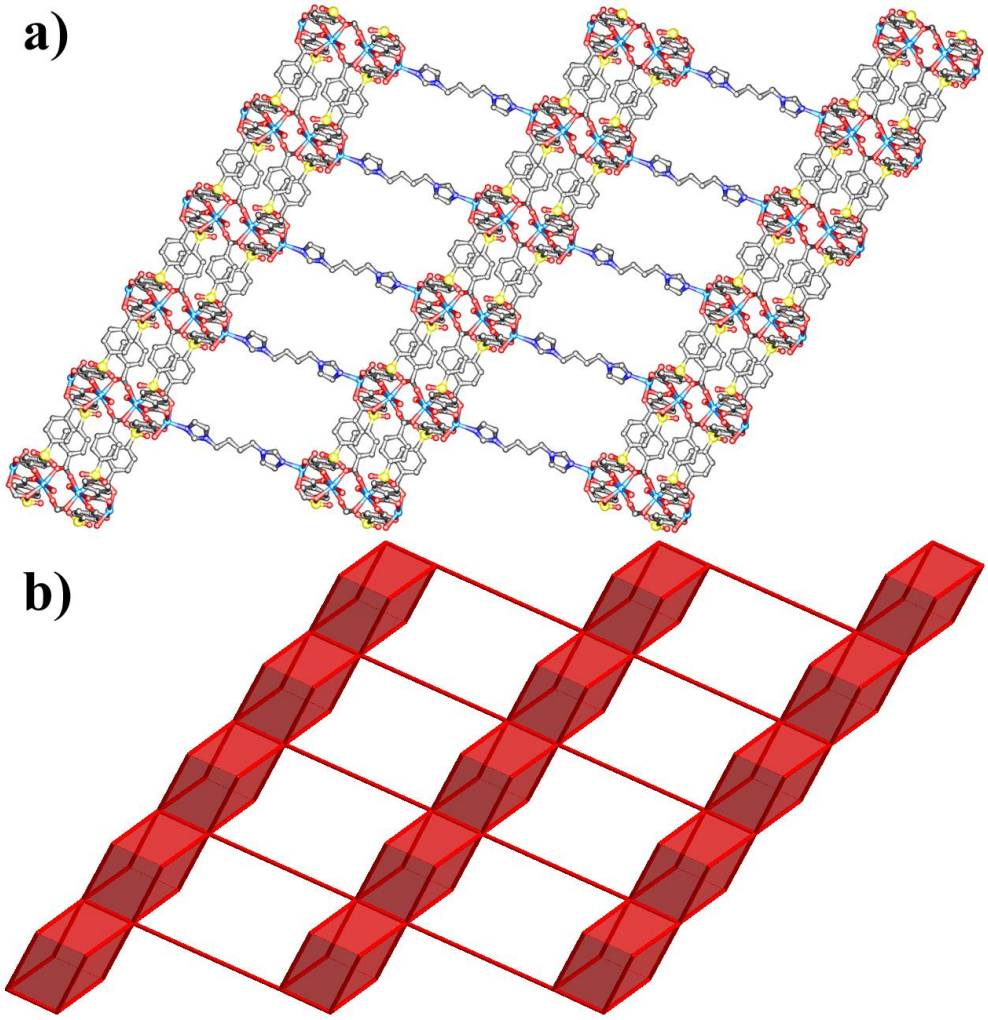

Fig. S15 Perspective (a) and schematic (b) views of a single 2D open framework of **3**.

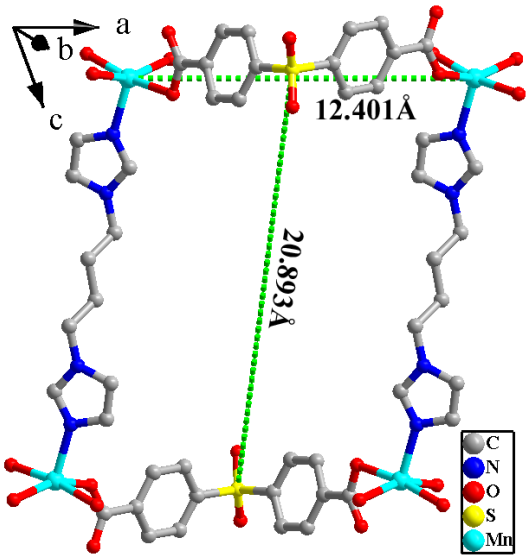

Fig. S16 Perspective view of a single tetragonal mesh of **3** with the relative dimensions 12.401 × 20.893 Å.

This journal is © The Royal Society of Chemistry 2011

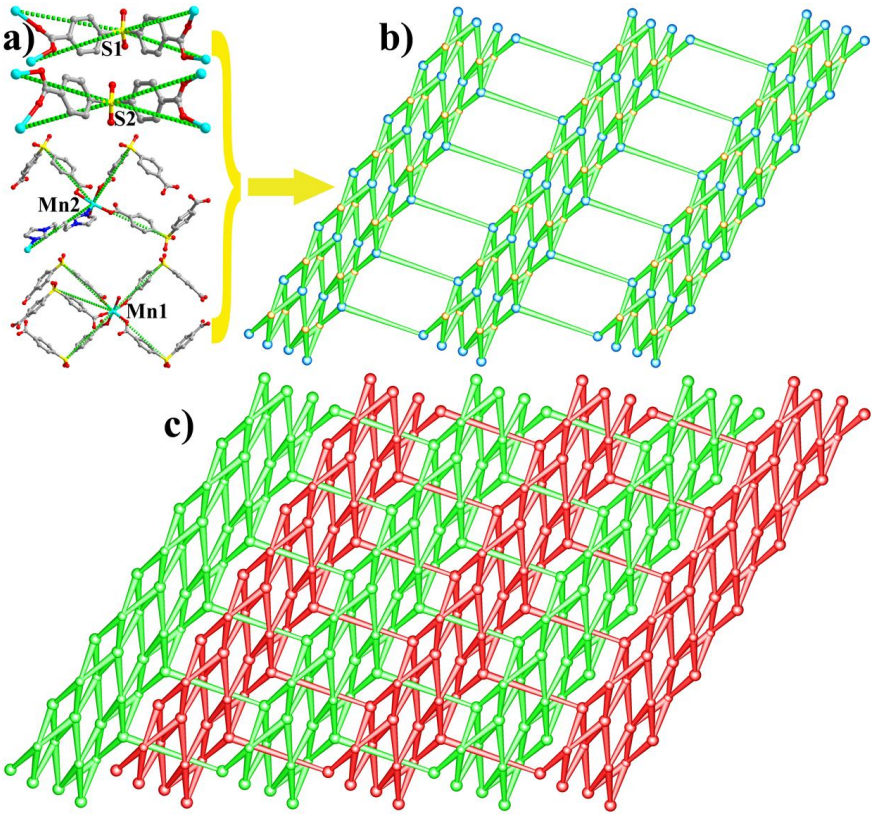

Fig. S17 (a) Perspective views of the four- and five-connected nodes in **3**. Green dashed lines illustrate the circumstance of each node (Mn atoms and sdba ligands). Schematic representation of (b) the single and (c) two interpenetrated 2D networks with tetranodal (4,5)-connected $(4^5.6)(4^4.6^2)(4^3.6^2.8)(4^6.6^4)$ topology of **3**.

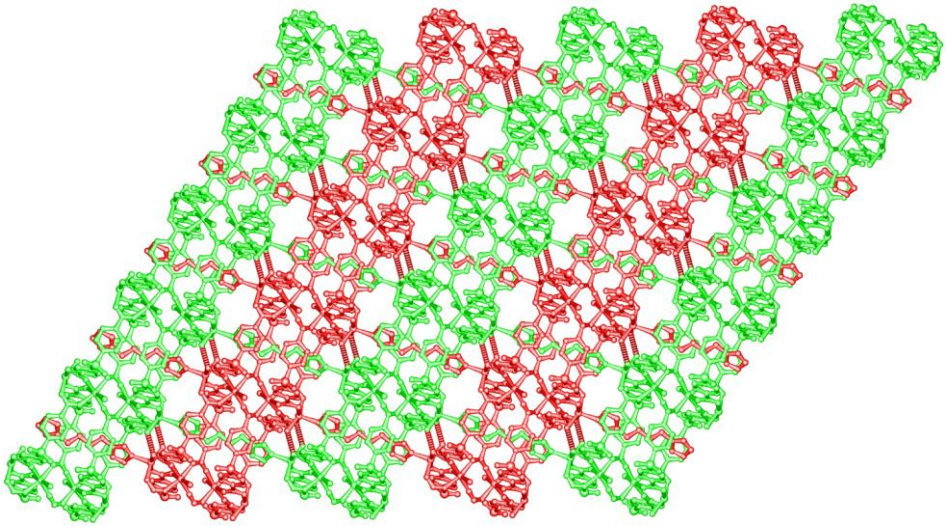

Fig. S18 Perspective view of the hydrogen bonding interactions (Ow(2)···O(10) 2.679(34) Å) between two interpenetrated 2D networks of **3**. The hydrogen bonds are indicated by red dashed lines.

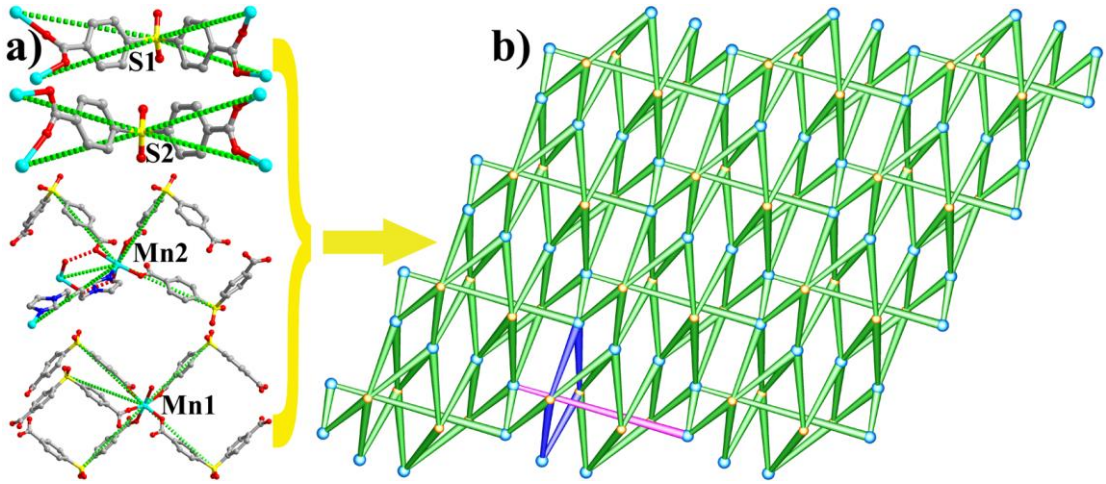

Fig. S19 (a) Perspective views of the four- and five-connected nodes in **3**. Red dashed lines illustrate the hydrogen bonds, green dashed lines illustrate the circumstance of each node (Mn atoms and sdba ligands). (b) Schematic representation of the tetranodal (4,5)-connected 2D self-penetrating network with $(4^5.6)(4^4.6^2)(4^3.6^4.8^3)(4^6.6^4)$ topology of **3**. The four-membered shortest ring is threaded by a rod of the same net, illustrating that this net is a self-penetrating one.

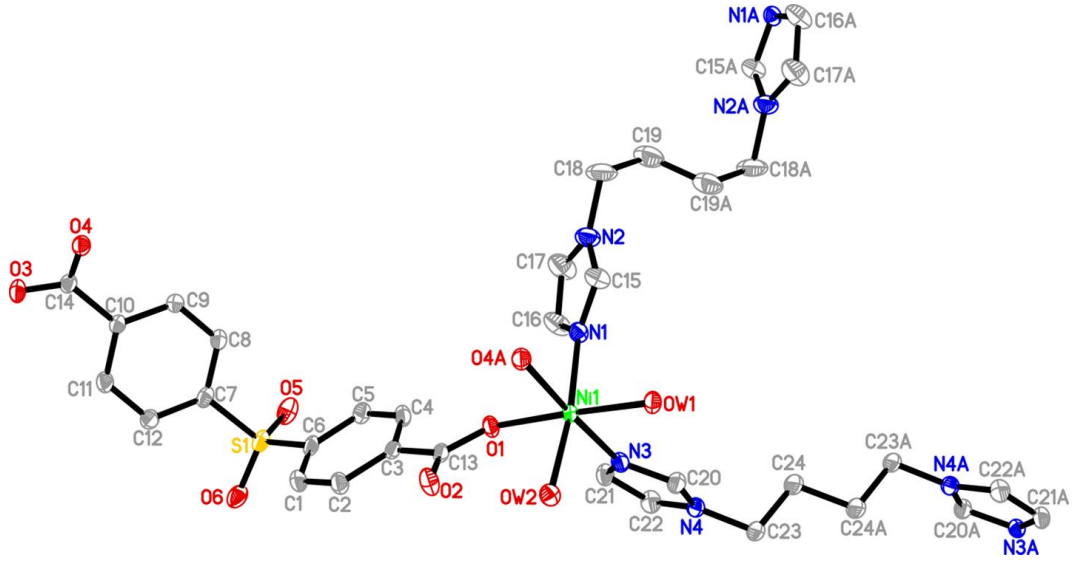

Fig. S20 ORTEP drawing of the coordination environment for Ni atom in **4** with thermal ellipsoids at the 30% probability level. The isolated water molecules and hydrogen atoms are omitted for clarity.

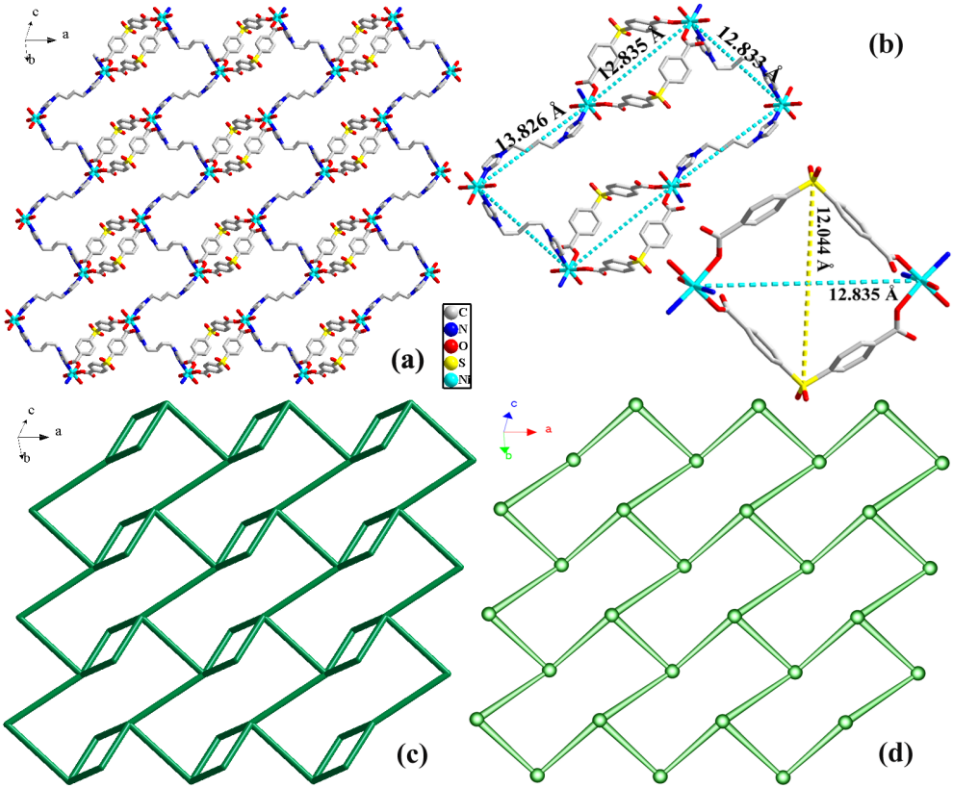

Fig. S21 Perspective views of (a) the single 2D framework of **4**, (b) the hexagonal ring with two "double-bridges" and the two-membered loop [$Ni_2(sdba)_2$] of approximate dimensions 13.826 × 12.835 × 12.833 Å and 12.835 × 12.044 Å, respectively. A schematic views of (c) the single 2D 4-connected framework with (2.6^5) topology of **4** and (d) the ordinary 3-connected 6^3 net.

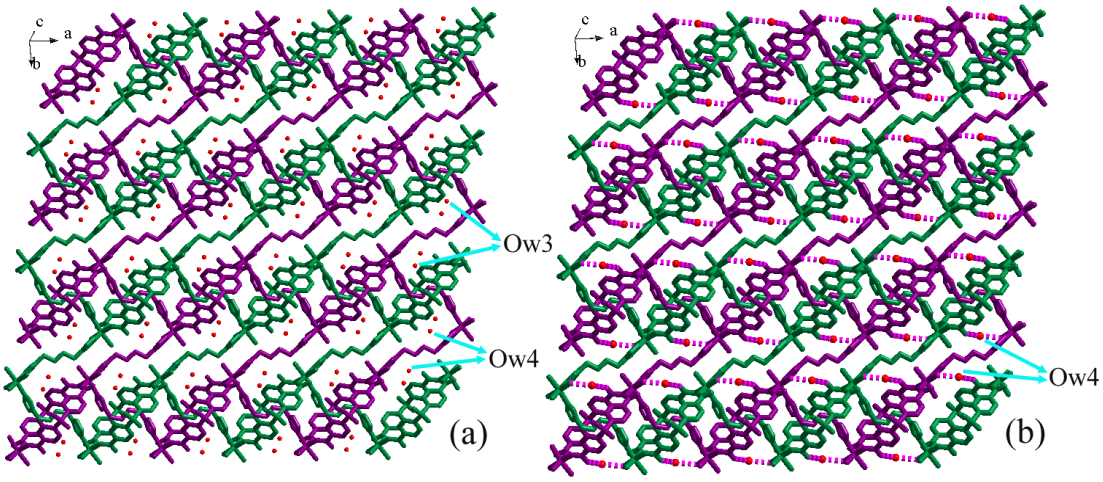

Fig. S22 Perspective views of (a) the free water molecules occupied by the voids of the overall entangled framework and (b) the hydrogen bonding interactions (Ow(4)···Ow(1) 2.756 Å, Ow(4)···O(2) 2.702 Å) between two interpenetrated 2D networks of **4**. The hydrogen bonds are highlighted by purple dashed lines.

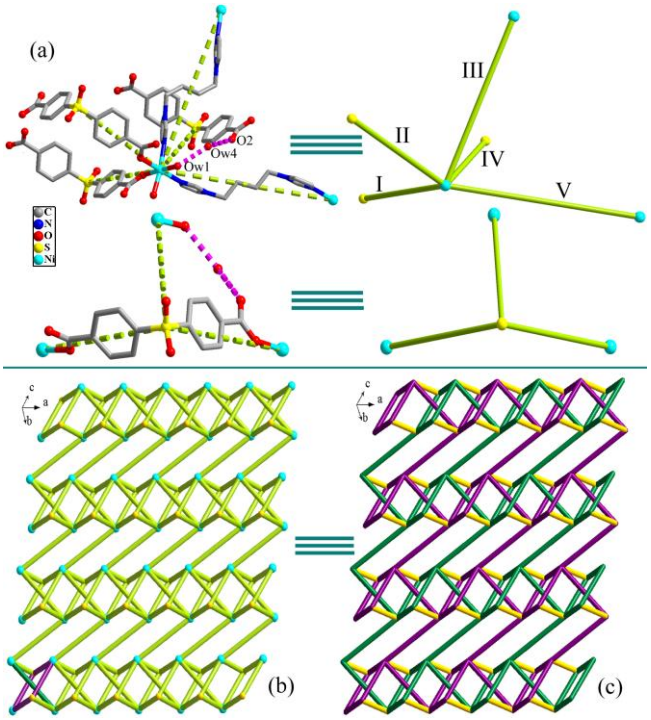

Fig. S23 (a) Perspective and simplified views of the five-connected Ni atom and three-connected sdba ligand in **4**. Purple dashed lines illustrate the hydrogen bonds. (b, c) Schematic presentations of (b) the binodal (3,5)-connected 2D self-penetrating network with $(4^2.5)(4^2.5^3.6^3.7^2)$ topology of **4**, which is derived from the crosslinked twofold interpenetrated 4-connected 2D (2.6^5) nets (c).

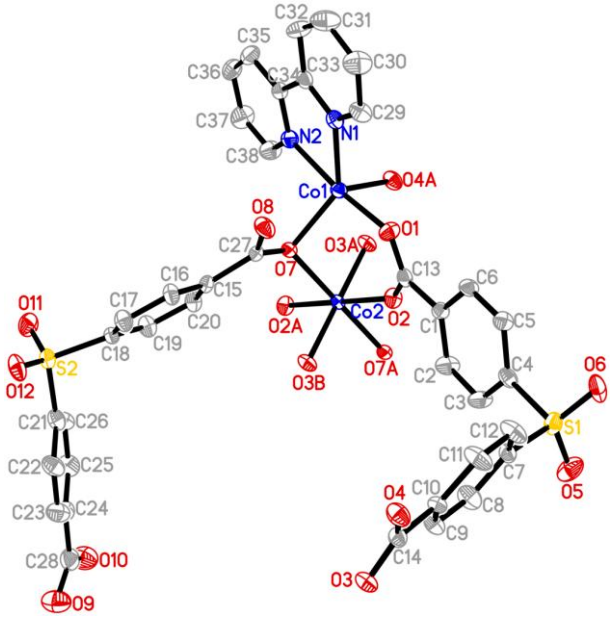

Fig. S24 ORTEP drawing of the coordination environment for Co atoms in **5** with thermal ellipsoids at the 30% probability level. The hydrogen atoms are omitted for clarity.

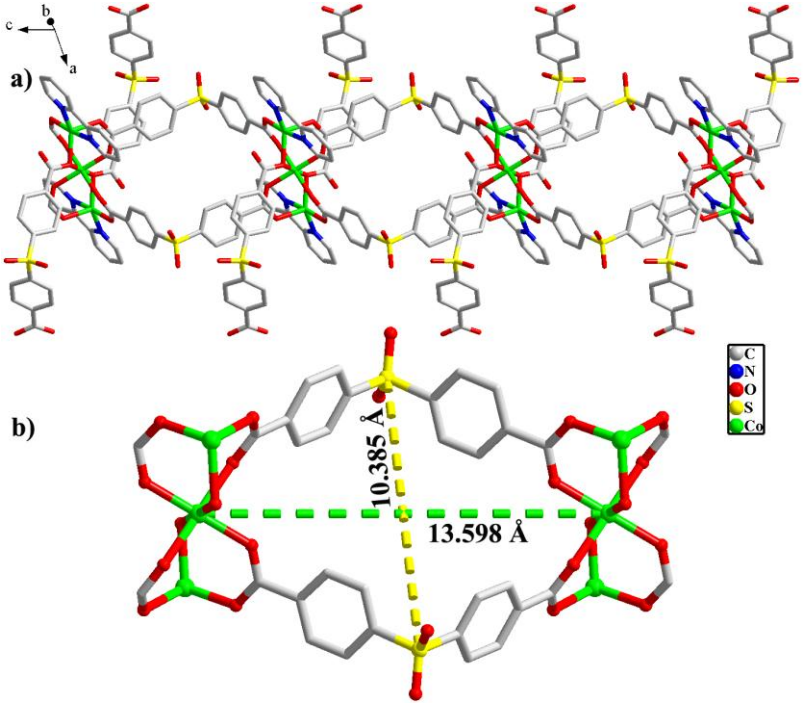

Fig. S25 Perspective views of (a) the 1D double-chain ribbons of **5** and (b) the $[Co_6(sdba)_2]$ loop with the relative dimensions 13.598 × 10.385 Å.

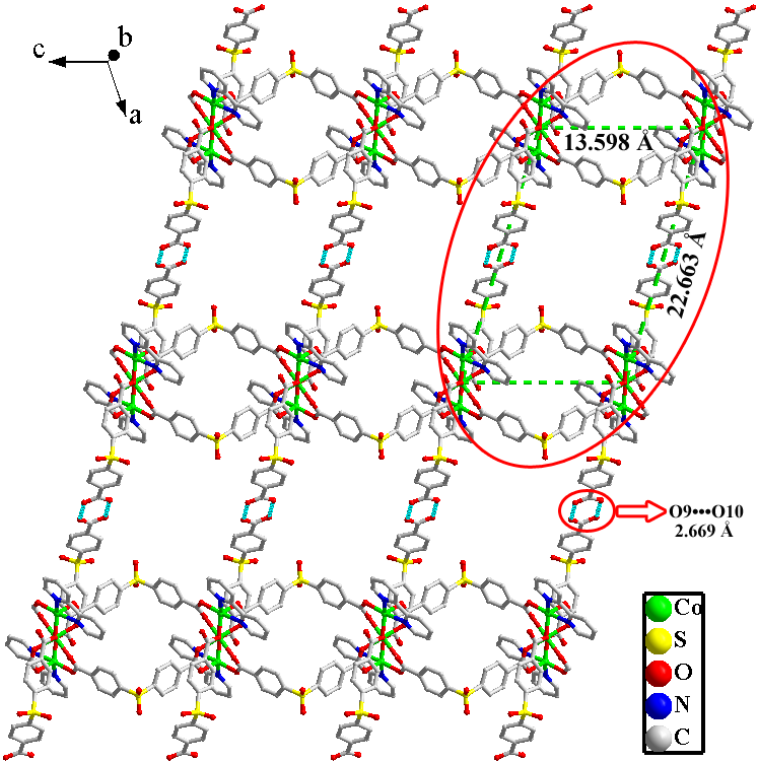

Fig. S26 Perspective view of a single 2D hydrogen-bonded layer of **5** that is formed when hydrogen bonds O(9)···O(10) (2.669 Å) are taken into account, in which the tetragonal mesh with large void of approximate dimensions 13.598 × 22.663 Å exists. The hydrogen bonds are highlighted by turquoise dashed lines.

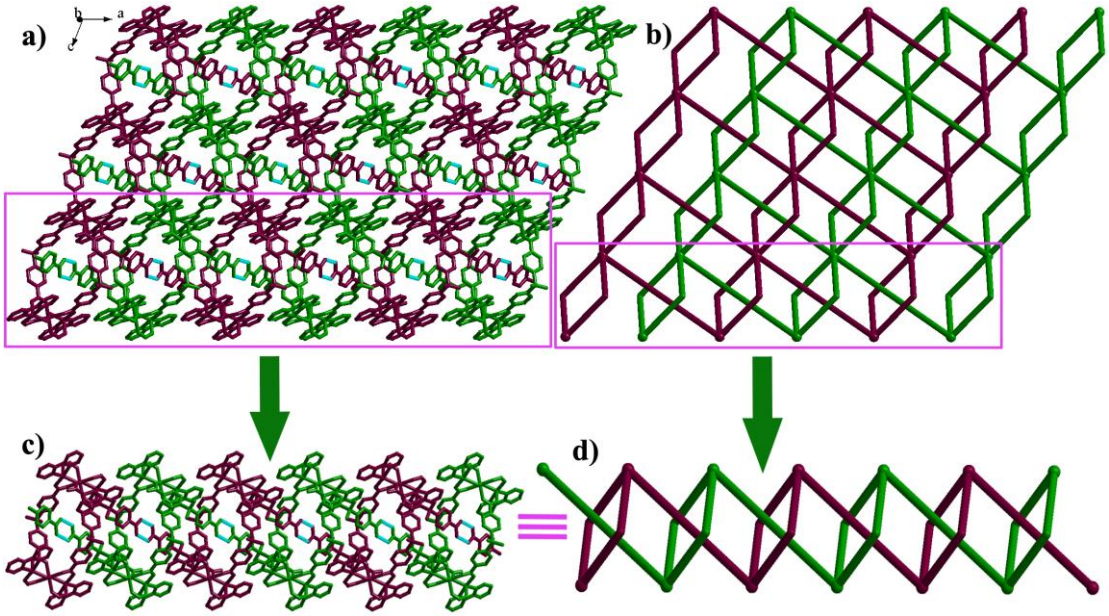

Fig. S27 Perspective and schematic views of (a, b) the two interpenetrated 2D hydrogen-bonded layers, and (c, d) the 1D hydrogen-bonded polyrotaxane column of **5**.

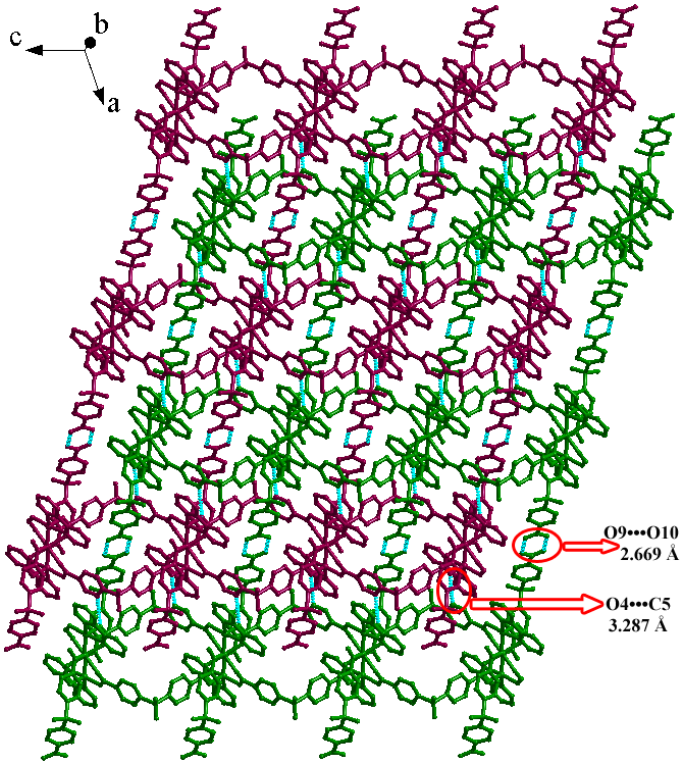

Fig. S28 Perspective view of the self-penetrating 2D hydrogen-bonded layer of **5** that is formed by when hydrogen bonds O(9)···O(10) (2.669 Å) and O(4)···C(5) (3.287 Å) are simultaneously taken into account. The hydrogen bonds are highlighted by turquoise dashed lines.

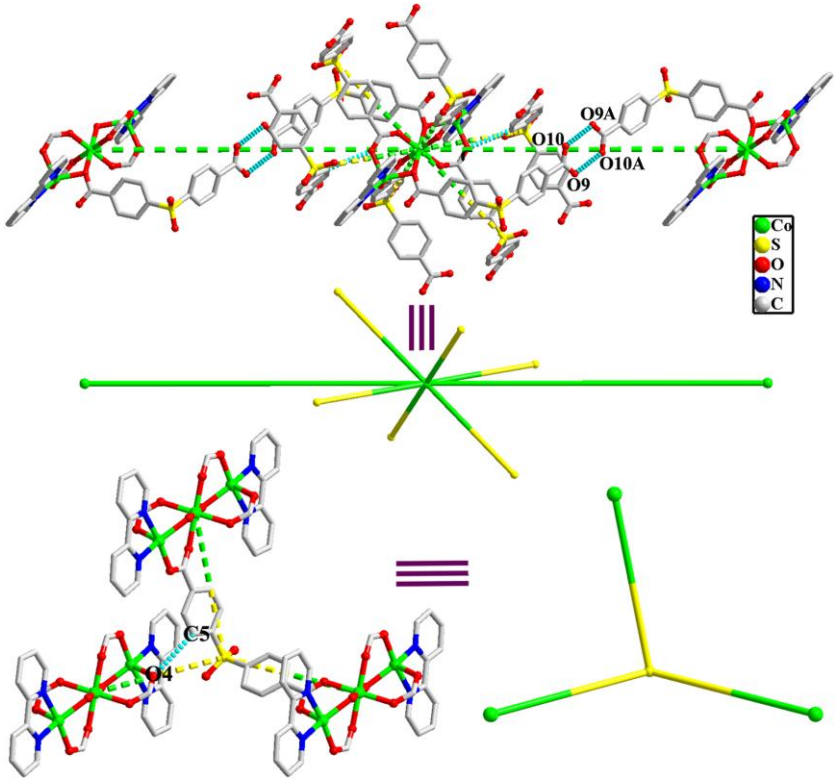

Fig. S29 Perspective and simplified views of the eight-connected trinuclear cobalt unit and three-connected sdba ligand in **5**. The hydrogen bonds O(9)···O(10) and O(4)···C(5) are both highlighted by turquoise dashed lines. (Symmetry transformations used to generate equivalent atoms: A = -2-x, -y, -1-z.)

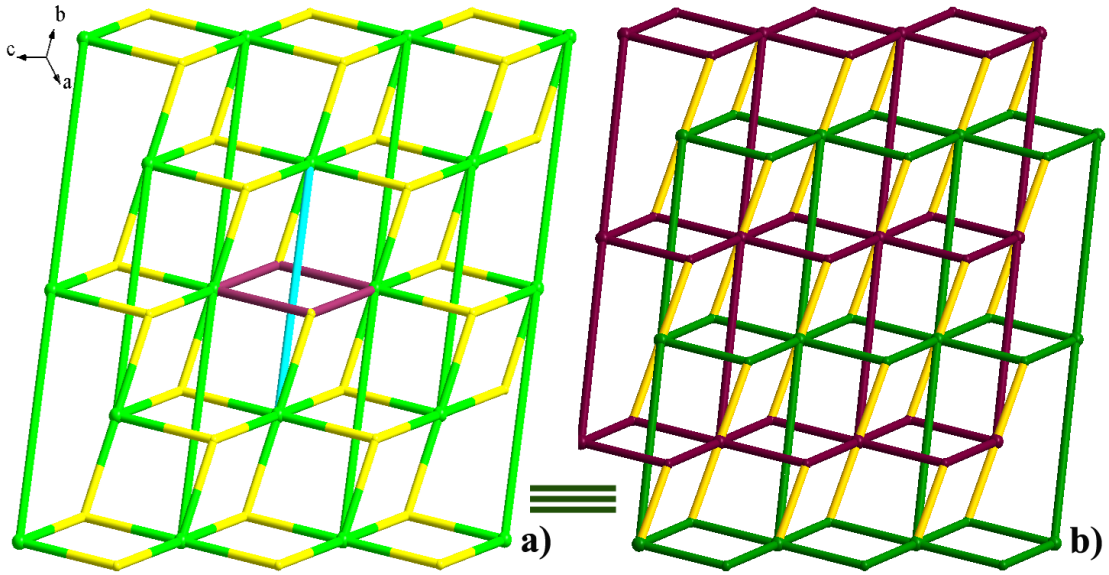

Fig. S30 Schematic presentations of (a) the binodal (3,8)-connected 2D self-penetrating network with $(4^3)_2(4^6.5^{11}.6^8.7^3)$ topology of **5**, which is derived from the crosslinked twofold interpenetrated 6-connected $(2^2.4^8.6^5)$ nets (b).

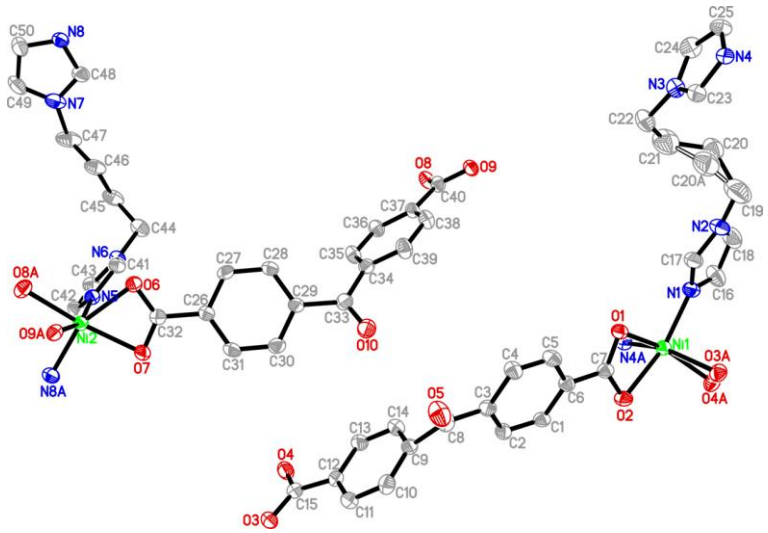

Fig. S31 ORTEP drawing of the coordination environment for Ni atoms in **6** with thermal ellipsoids at the 30% probability level. The isolated water molecules and hydrogen atoms are omitted for clarity.

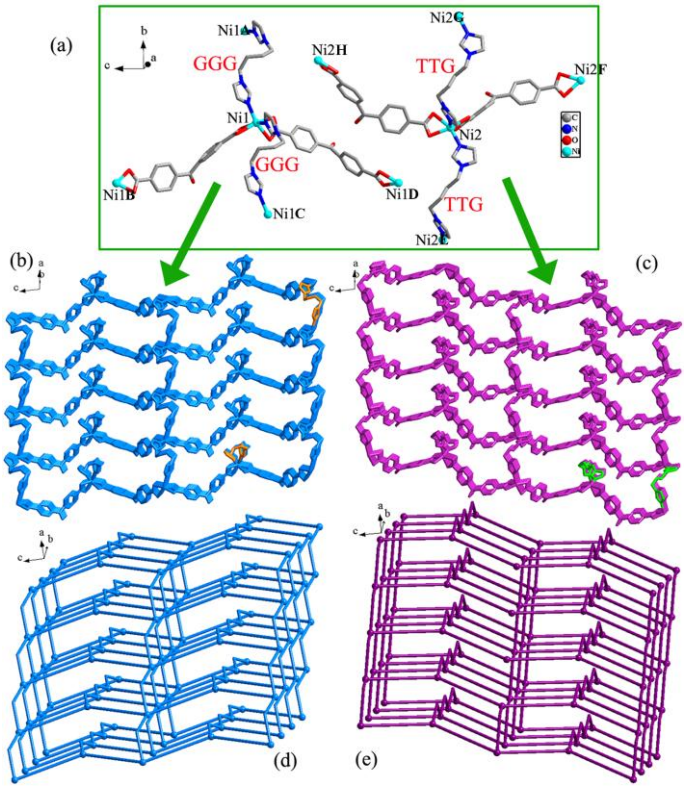

Fig. S32 (a) Perspective view of the difference between crystallographically Ni1 and Ni2 units in **6**. (Symmetry transformations used to generate equivalent atoms: A = -0.5+x, 0.5+y, z; B = x, -y, 0.5+z; C = 0.5+x, -0.5+y, z; D = x, -y, -0.5+z; E = -0.5+x, -0.5+y, z; F = -0.5+x, 0.5-y, -0.5+z; G = 0.5+x, 0.5+y, z; H = 0.5+x, 0.5-y, 0.5+z.) Perspective (b, c) and simplified (d, e) views of two crystallographically distinct 3D

This journal is © The Royal Society of Chemistry 2011

networks both with $CdSO_4$ topology.

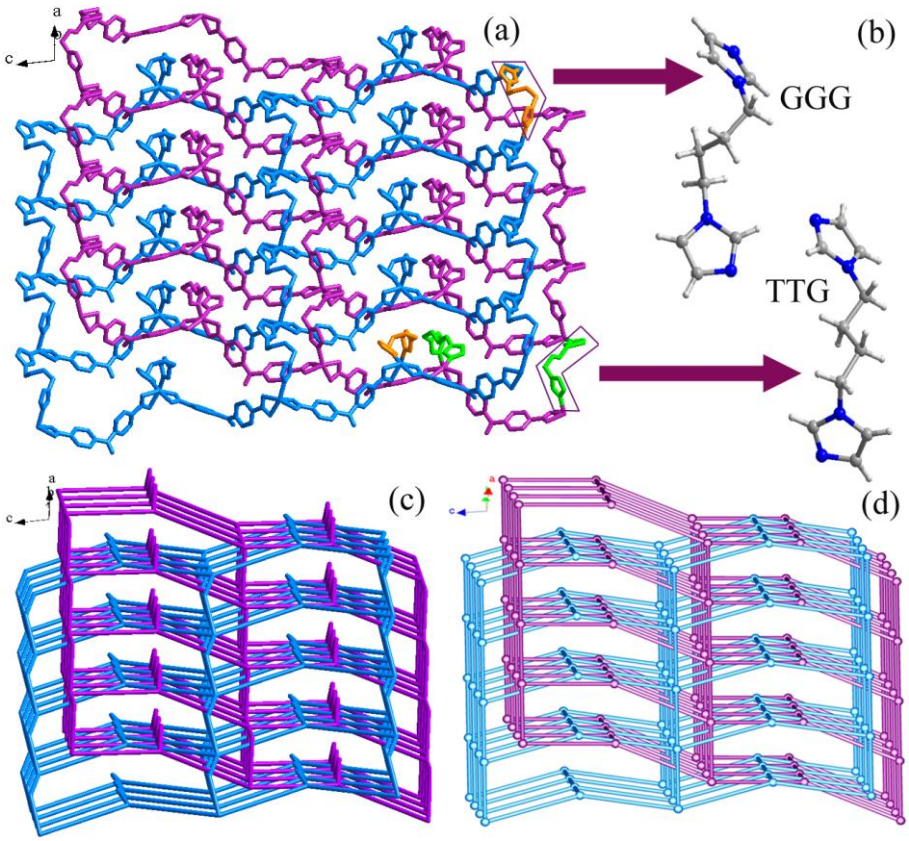

Fig. S33 Perspective (a) and schematic (c, d) views of the interpenetration of two distinct 3D networks both with $CdSO_4$ topology. (b) The two different kinds of configuration of bim ligands in **6**.

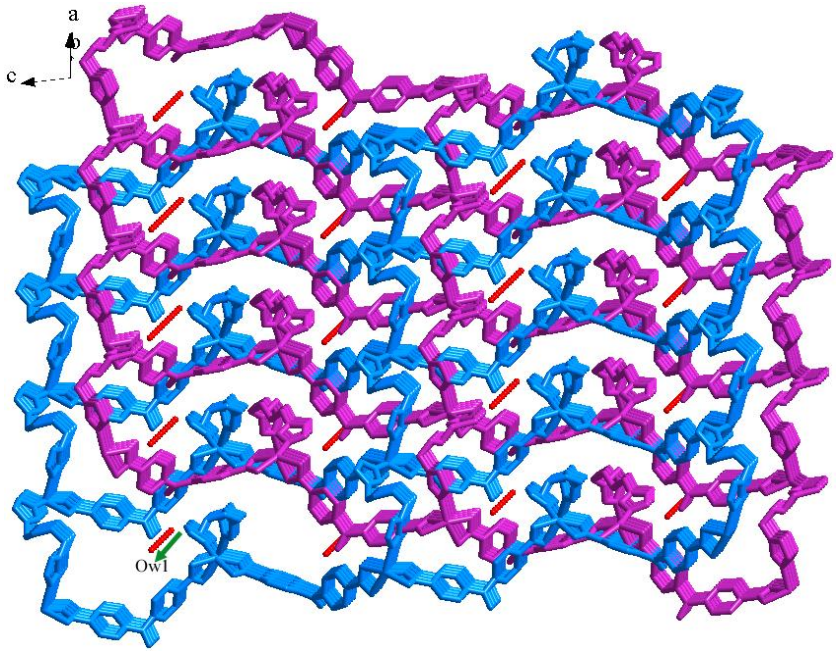

Fig. S34 Perspective view of the free water molecules occupied by the voids of the

overall entangled framework of **6**.

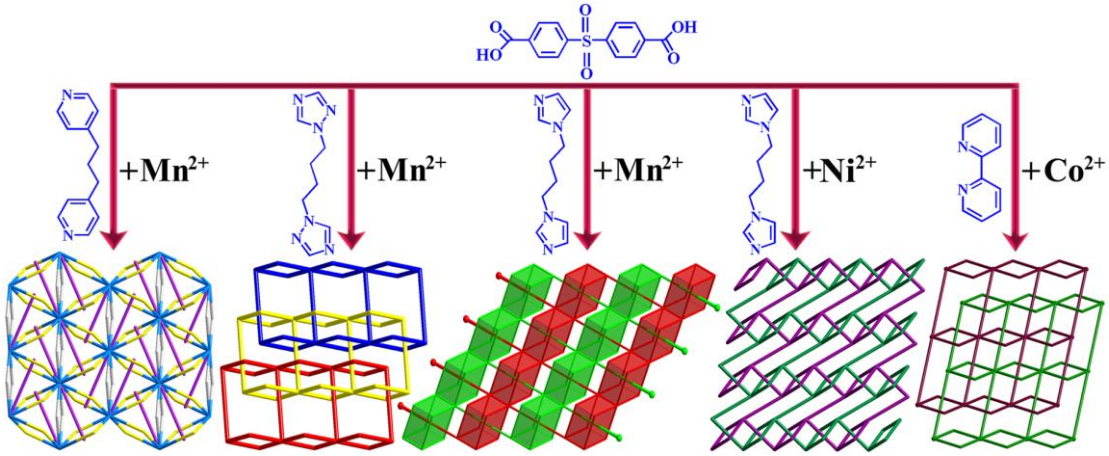

Fig. 35 Schematic views of compounds **1**-**5** in this work.

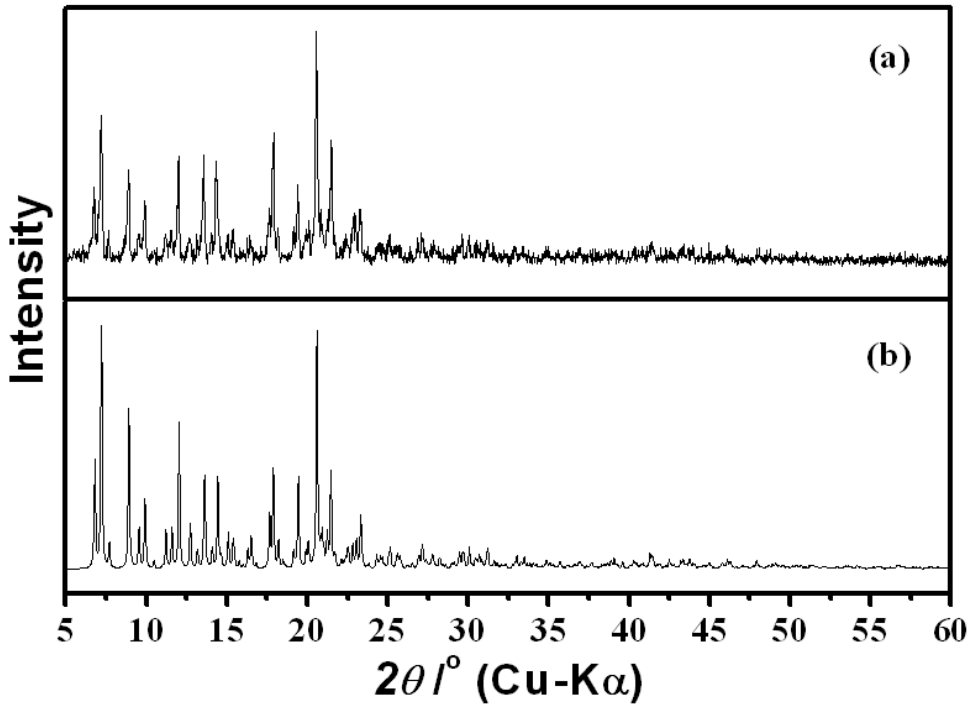

Fig. S36 The XRPD patterns for: (a) as-synthesized samples of **1**, and (b) simulated one based on the single-crystal structure of **1**.

This journal is © The Royal Society of Chemistry 2011

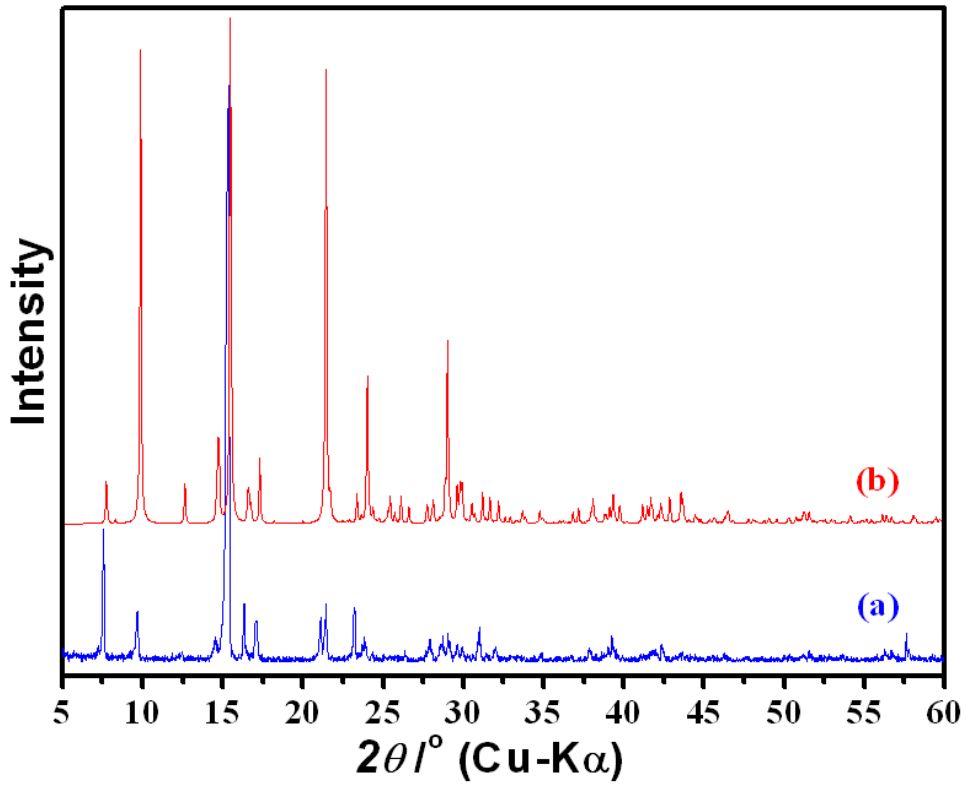

Fig. S37 The XRPD patterns for: (a) as-synthesized samples of **2** (blue), and (b) simulated one based on the single-crystal structure of **2** (red).

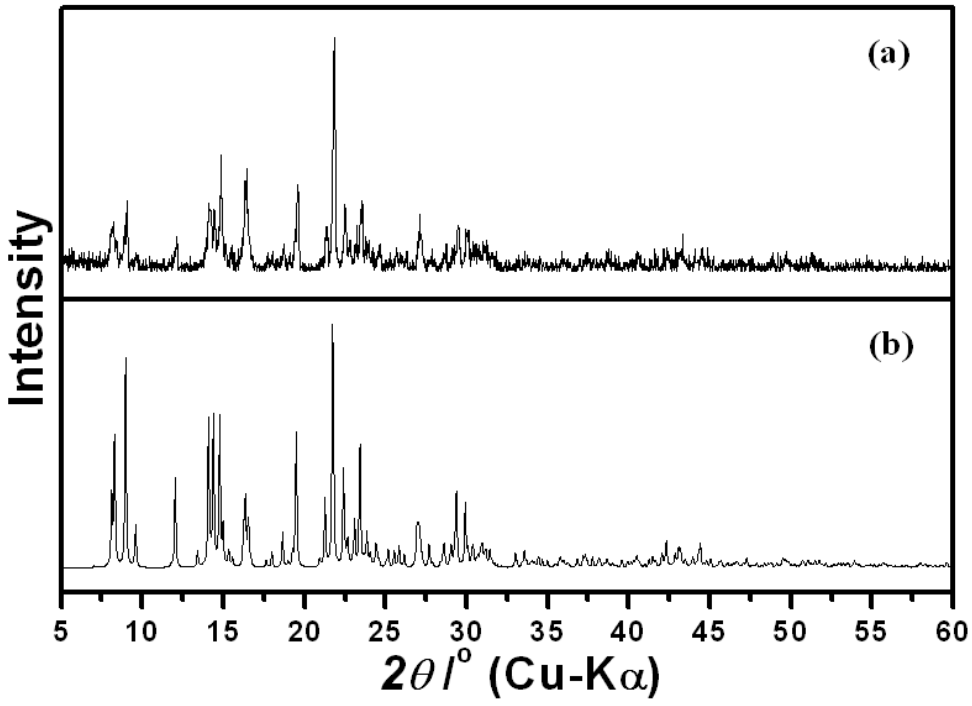

Fig. S38 The XRPD patterns for: (a) as-synthesized samples of **3**, and (b) simulated one based on the single-crystal structure of **3**.

This journal is © The Royal Society of Chemistry 2011

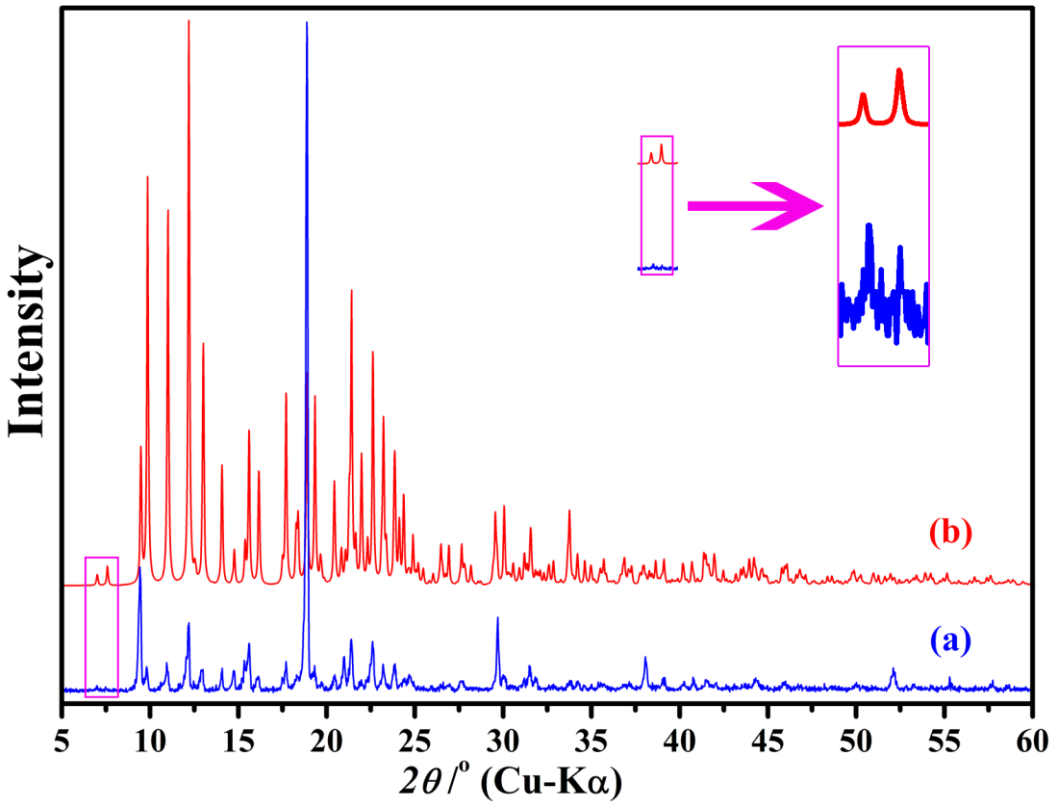

Fig. S39 The XRPD patterns for: (a) as-synthesized samples of **4** (blue), and (b) simulated one based on the single-crystal structure of **4** (red).

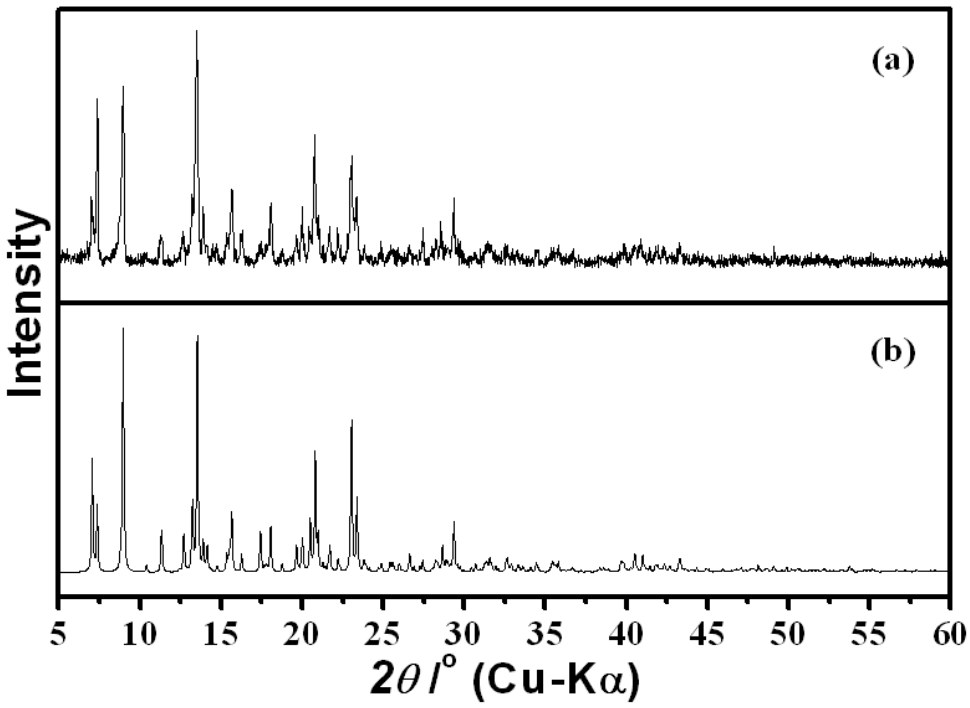

Fig. S40 The XRPD patterns for: (a) as-synthesized samples of **5**, and (b) simulated one based on the single-crystal structure of **5**.

This journal is © The Royal Society of Chemistry 2011

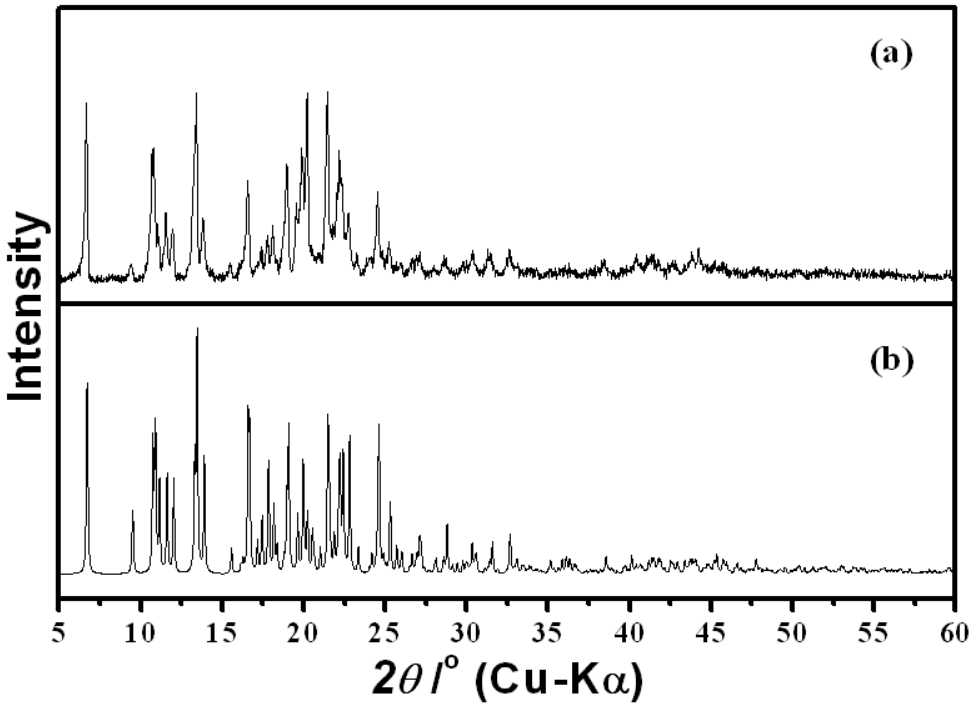

Fig. S41 The XRPD patterns for: (a) as-synthesized samples of **6**, and (b) simulated one based on the single-crystal structure of **6**.

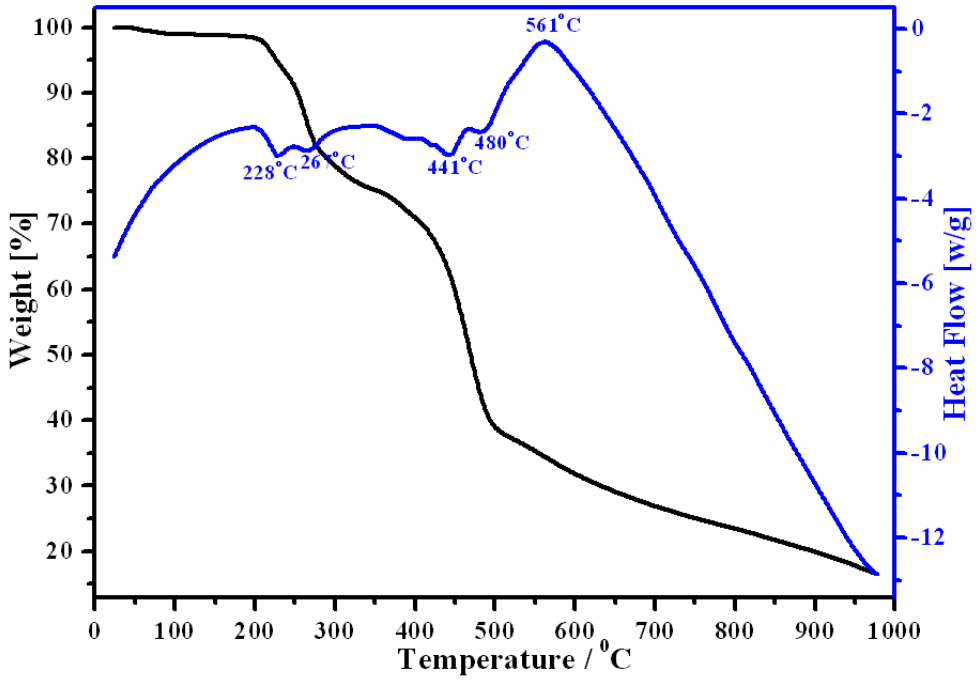

Fig. S42 The TG-DSC curves of compound **1**.

This journal is © The Royal Society of Chemistry 2011

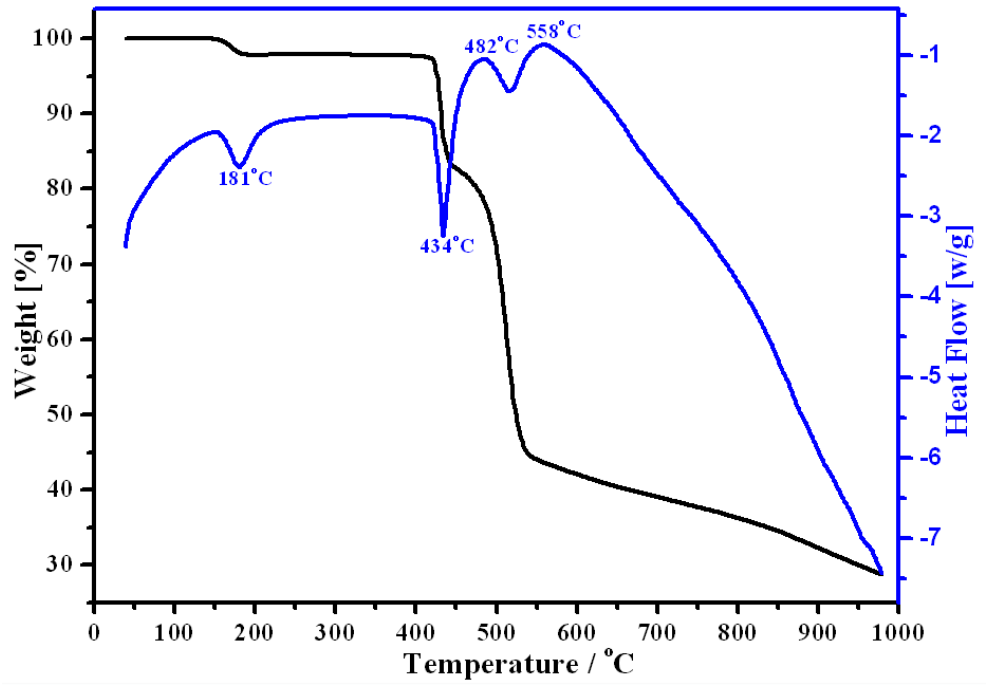

Fig. S43 The TG-DSC curves of compound **2**.

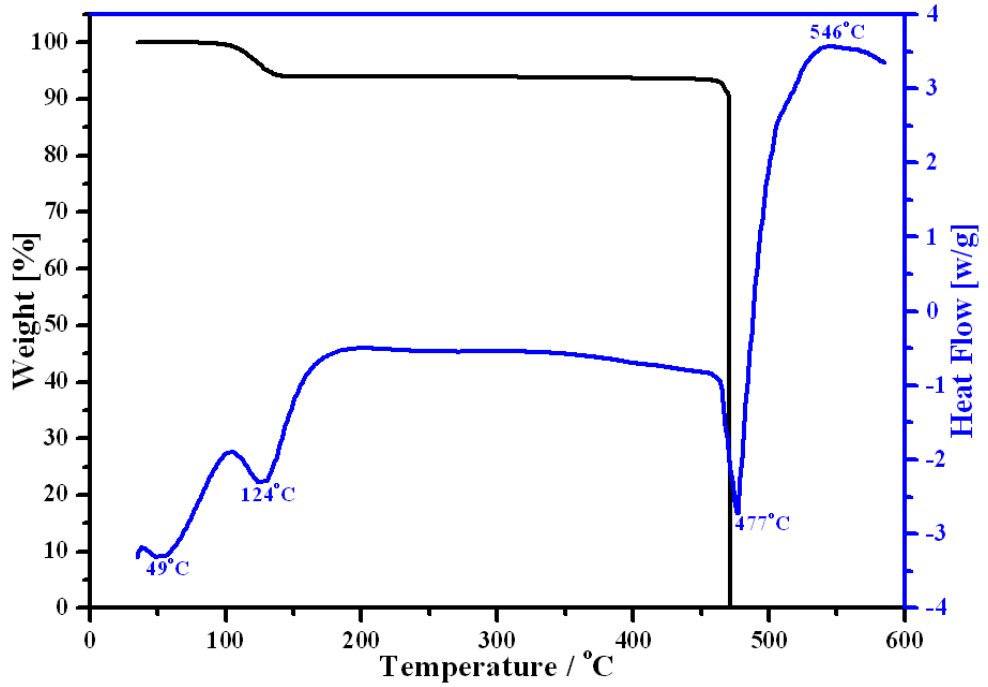

Fig. S44 The TG-DSC curves of compound **3**.

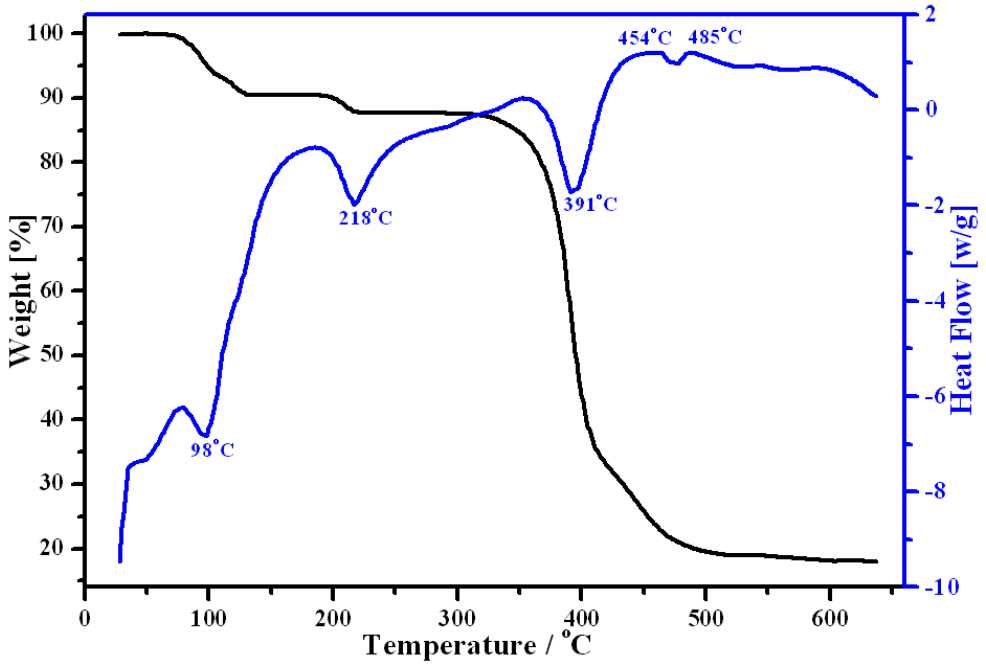

Fig. S45 The TG-DSC curves of compound **4**.

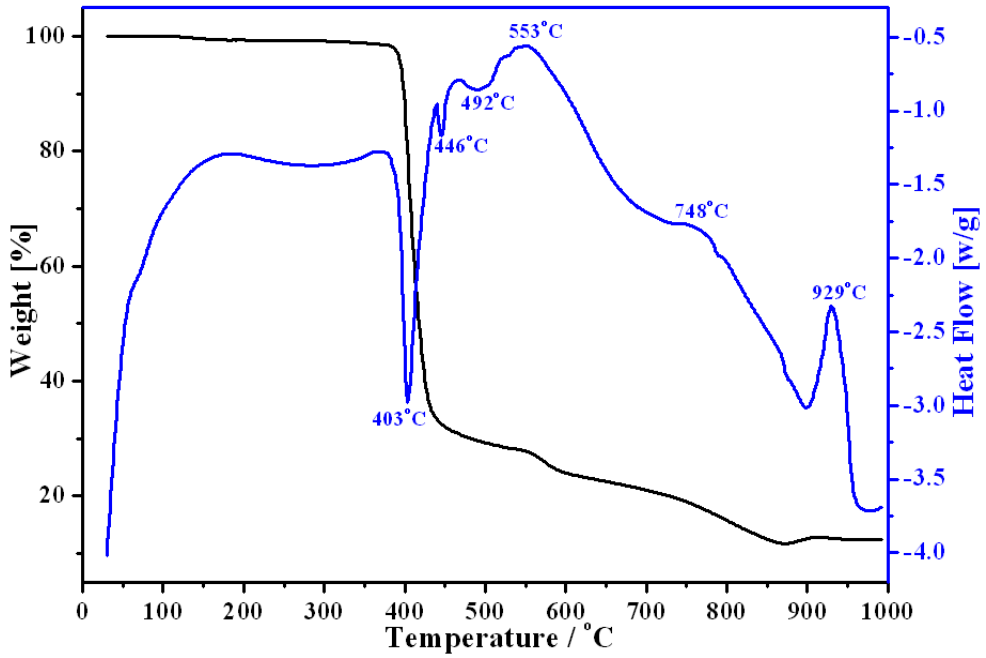

Fig. S46 The TG-DSC curves of compound **5**.

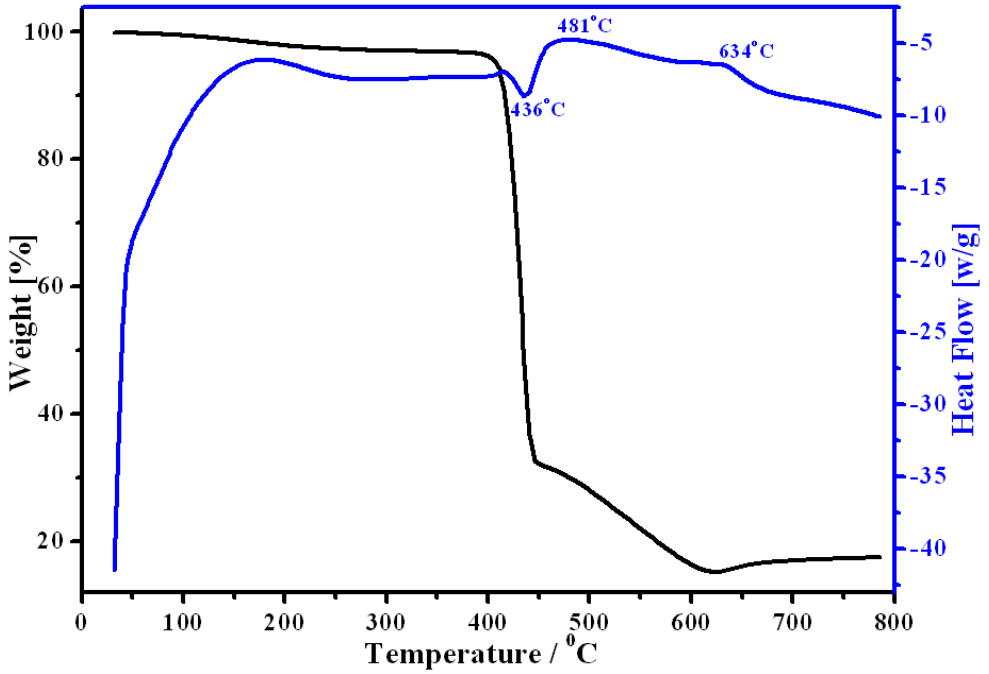

Fig. S47 The TG-DSC curves of compound **6**.

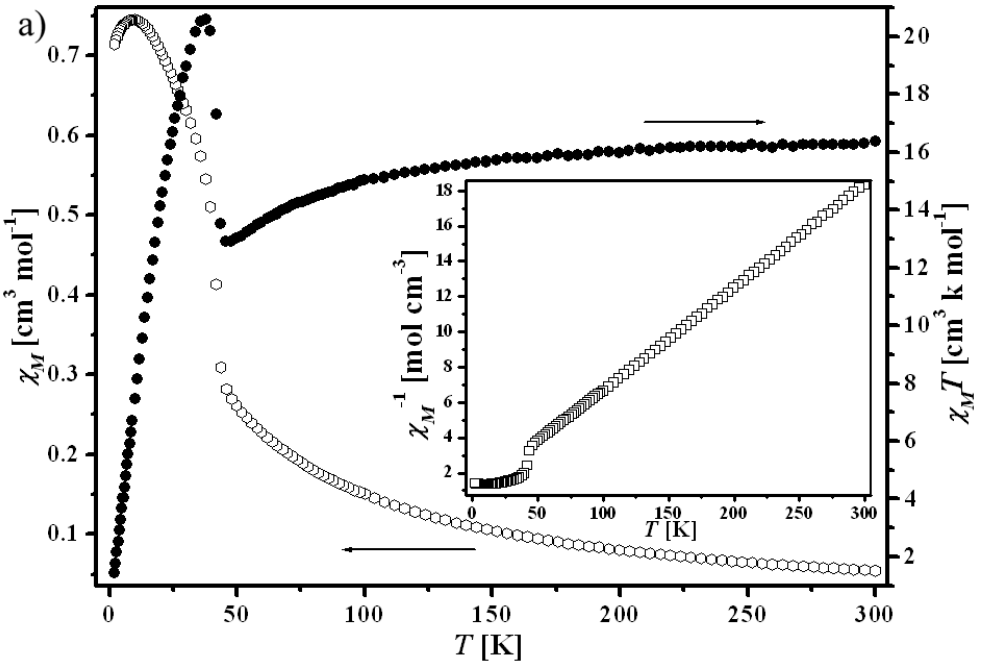

Fig. S48 Thermal variation of χ_M and $\chi_M T$ for compounds **1**. Insert: Plot of thermal variation of χ_M^{-1} for compound **1**.

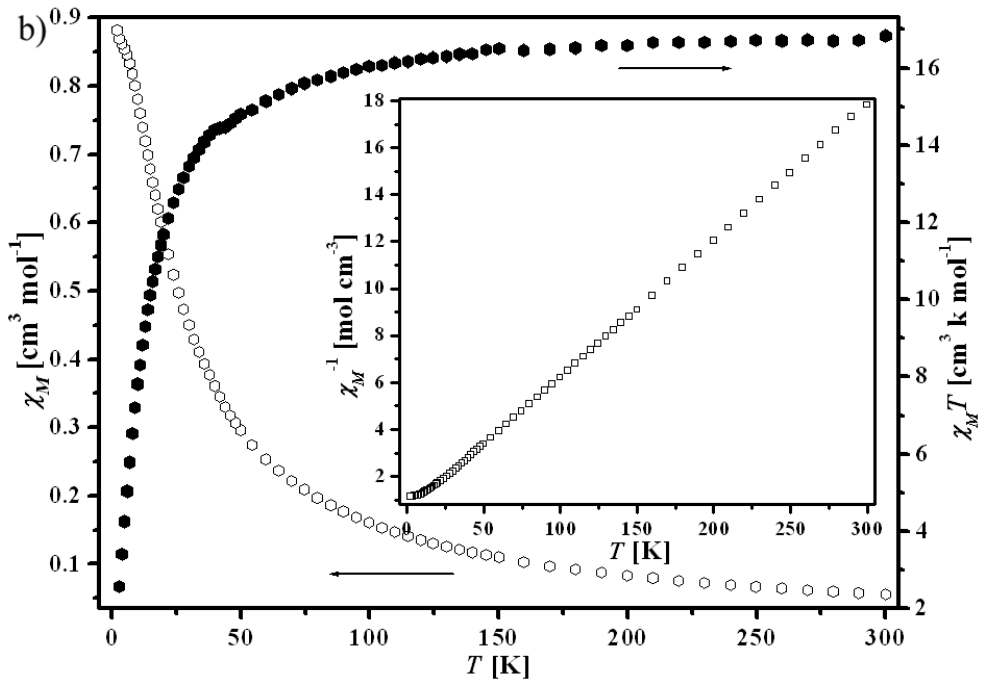

Fig. S49 Thermal variation of χ_M and $\chi_M T$ for compounds **3**. Insert: Plot of thermal variation of χ_M^{-1} for compound **3**.

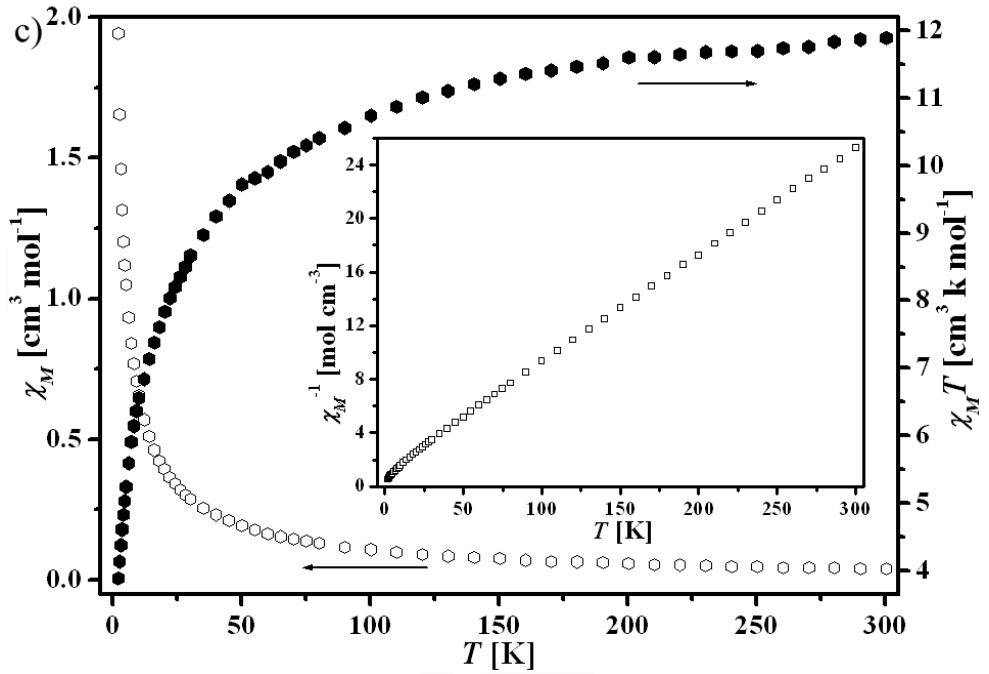

Fig. S50 Thermal variation of χ_M and $\chi_M T$ for compounds **5**. Insert: Plot of thermal variation of χ_M^{-1} for compound **5**.

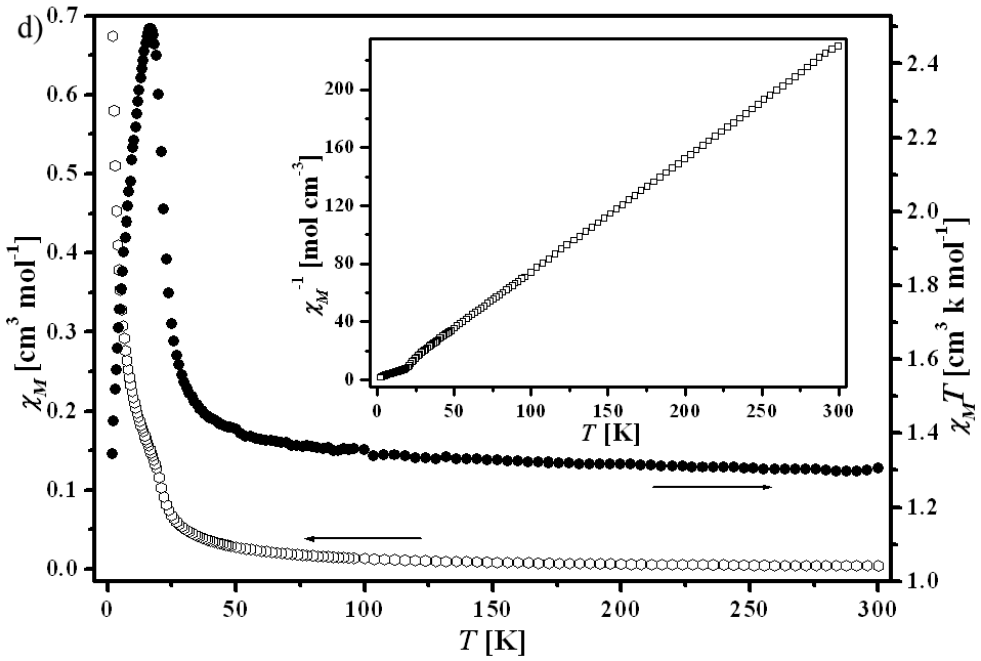

Fig. S51 Thermal variation of χ_M and $\chi_M T$ for compounds **4**. Insert: Plot of thermal variation of χ_M^{-1} for compound **4**.

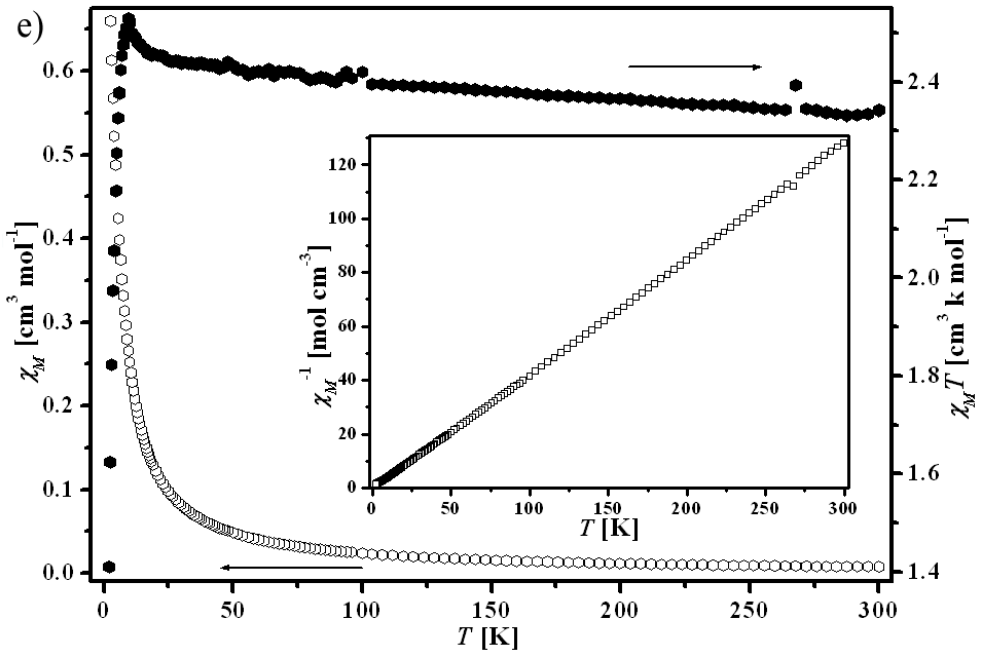

Fig. S52 Thermal variation of χ_M and $\chi_M T$ for compounds **6**. Insert: Plot of thermal variation of χ_M^{-1} for compound **6**.

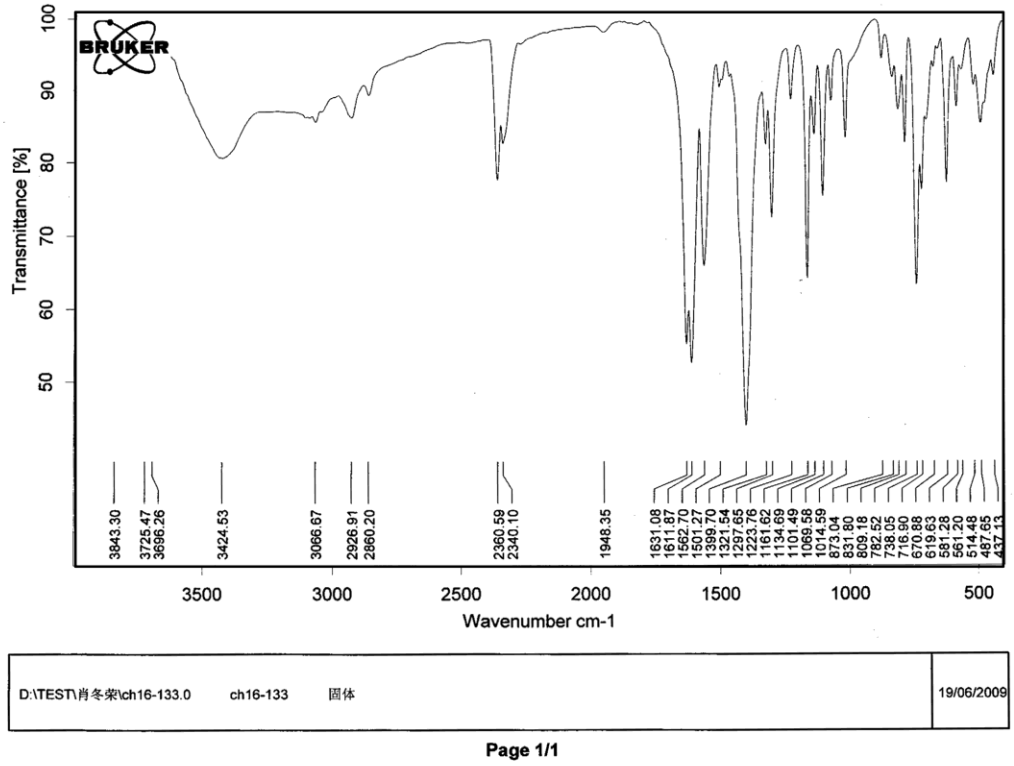

Fig. S53 The IR spectrum of compound **1**.

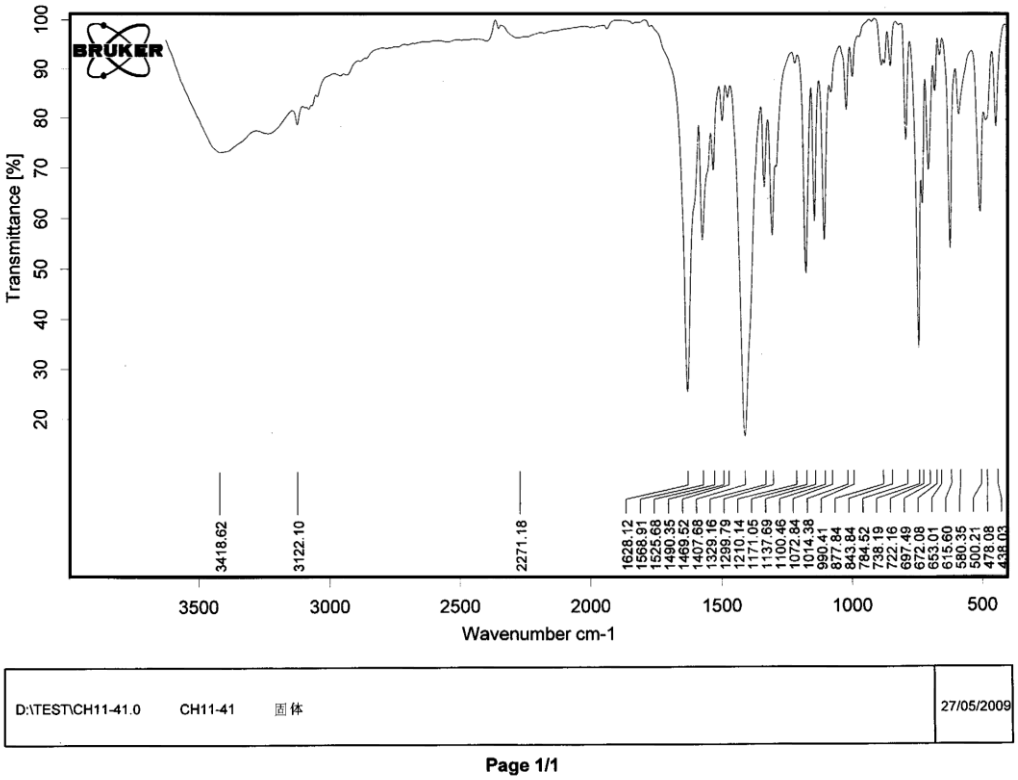

Fig. S54 The IR spectrum of compound **2**.

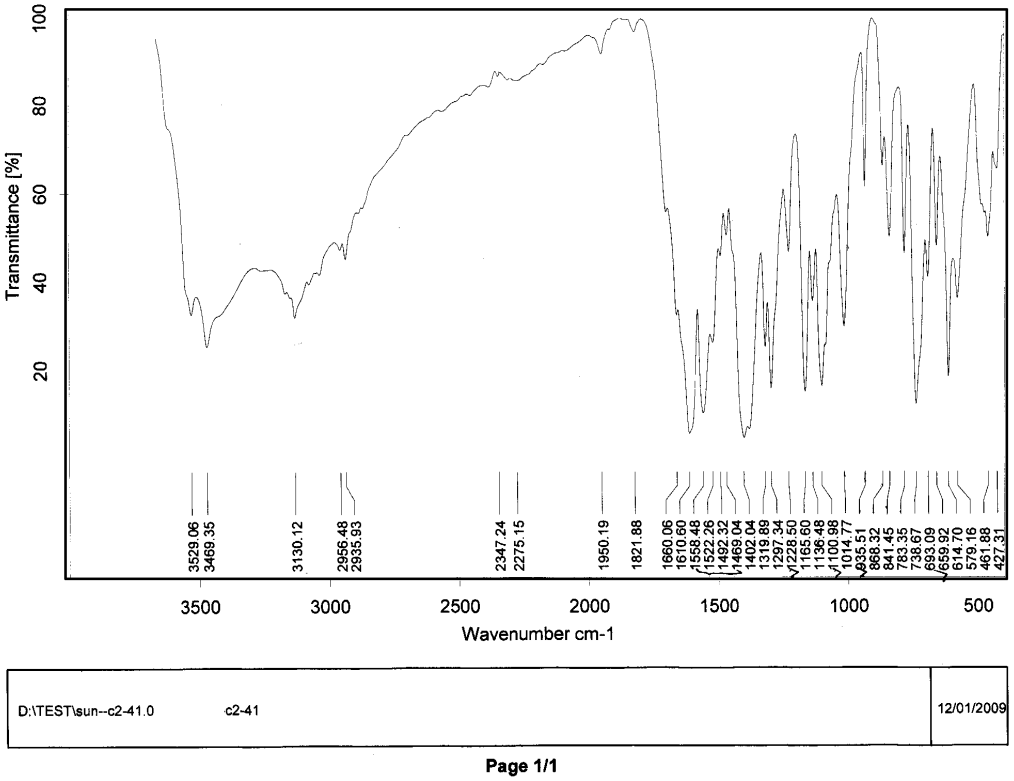

Fig. S55 The IR spectrum of compound **3**.

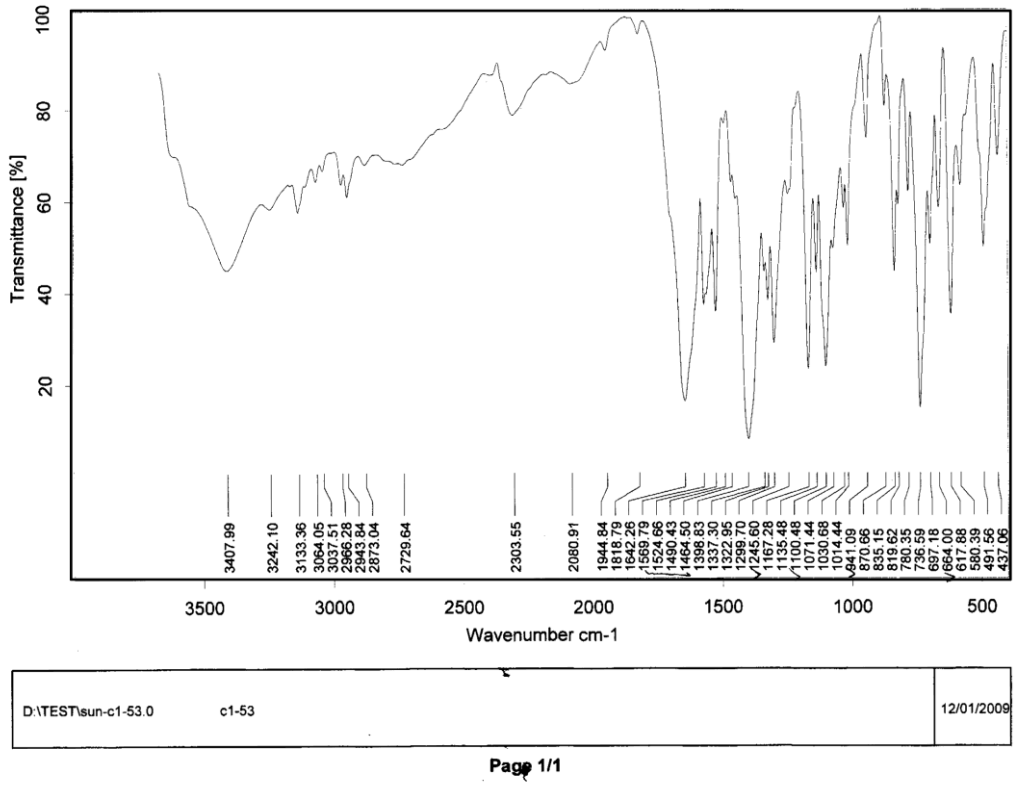

Fig. S56 The IR spectrum of compound **4**.

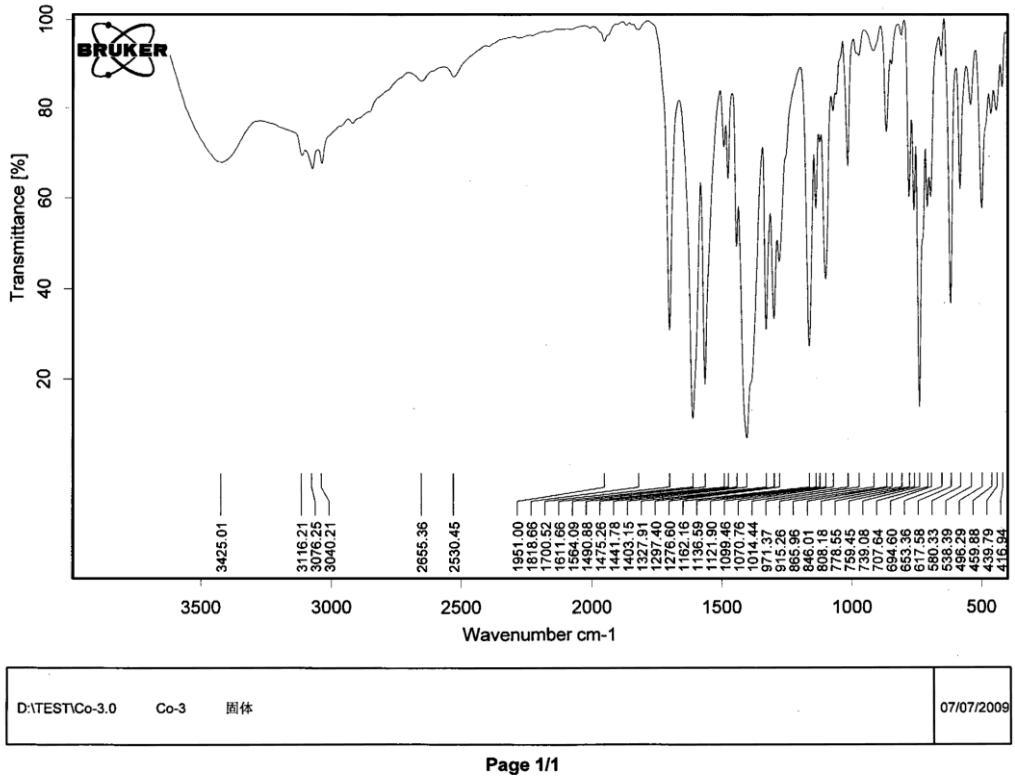

Fig. S57 The IR spectrum of compound **5**.

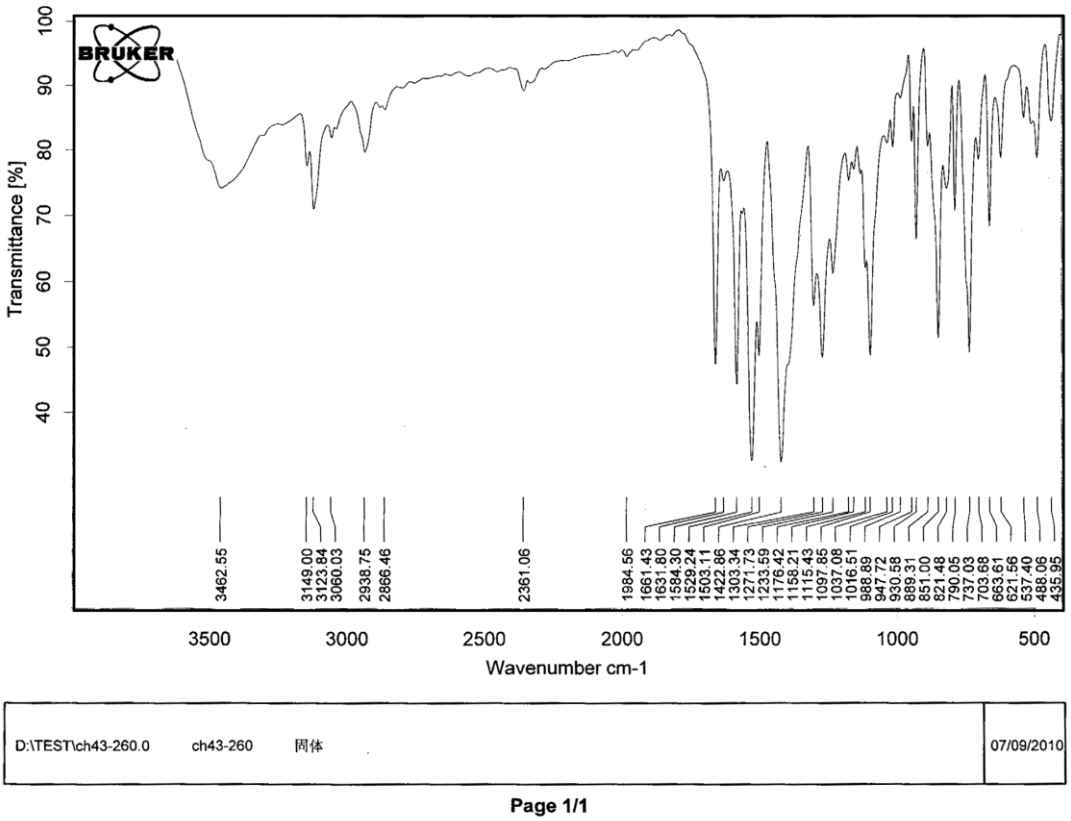

Fig. S58 The IR spectrum of compound **6**.

This journal is © The Royal Society of Chemistry 2011

Additional details for single-crystal structural refinements

In the process of structure refinement of **1**, it was found that some carbon atoms of the $(CH_2)_3$ chains (C11, C12, C13) and pyridyl rings (C1, C2, C3, C19, C20, C22, C23) in the two crystallographically independent bpp ligands are disordered. They were refined with the help of restraints on bond distances (C-C and C-N) and displacement parameters, as well as by treating restrained comments "FLAT" for the disorder pyridyl rings (N4, C19A, C20A, C21, C22A, C23A) to make the geometry of the bpp ligand close to ideal. The relative occupancies for the disordered components were refined with a total occupancy of 1. The restrained refinement comment "ISOR" is used during the refinement to restraint the Non-H atoms with the ADP problems, these atoms are as follows: C1, C2, C3, C1A, C2A, C3A, C6, C7, C10, C11, C12, C13, C15, C11A, C12A, C13A, C19A, C20A, C22A, C23A, C25, N2 in **1**. The chemically equivalent O-H and non-bonding H···H distances within the H_2O molecules were also refined with the help of distance restraints.

In the process of structure refinement of **2**, some carbon atoms (C15, C17, C18) of btb ligand were disordered over two positions that were related by the internal mirror plane of crystal, and yet one carboxylic group (C14, O3, O4) and some phenyl carbon atoms (C8, C9, C10, C11) of sdba ligand were disordered over two positions. These disordered atoms were modeled by application of distance restraints for chemically equivalent bonding and non-bonding interactions (C-C, C-N and C···C), and were refined with restrained comments "DELU" and "SIMU" to be sure that all the atoms have the similar environment. The relative occupancies for the disordered components were refined with a total occupancy of 1. The restrained refinement comment "ISOR" is also used during the refinement to restraint the Non-H atoms with the ADP problems, these atoms are as follows: C8, C9, C10, C11, C14, C8A, C9A, C10A, C11A, C14A, C15, C16, C18, O3, O3A, O4, O4A in **2**.

In the process of structure refinement of **3**, fifteen restraints were used in the refinement. The chemically equivalent O-H and non-bonding H···H distances within the H_2O molecules were refined with the help of distance restraints. Whereas, a

This journal is © The Royal Society of Chemistry 2011

restrained refinement comment "ISOR" is used to restraint the Non-H atoms with the ADP problems in **3**.

In the process of structure refinement of **4**, fifteen restraints were used in the refinement. The chemically equivalent O-H and non-bonding H···H distances within the H_2O molecules were refined with the help of distance restraints. Whereas, a restrained refinement comment "ISOR" is used to restraint the Non-H atoms with the ADP problems in **4**.

In the process of structure refinement of **6**, the C20 atom of one bim ligand was disordered over two positions. During the refinement, the disordered atom was modeled by application of distance restraints for chemically equivalent bonding interactions (C-C bonds). The relative occupancies for the disordered atom were refined with a total occupancy of 1. The restrained refinement comment "ISOR" is also used to restraint the Non-H atoms with the ADP problems, these atoms are as follows: C19, C20, C20A, C21 in **6**.